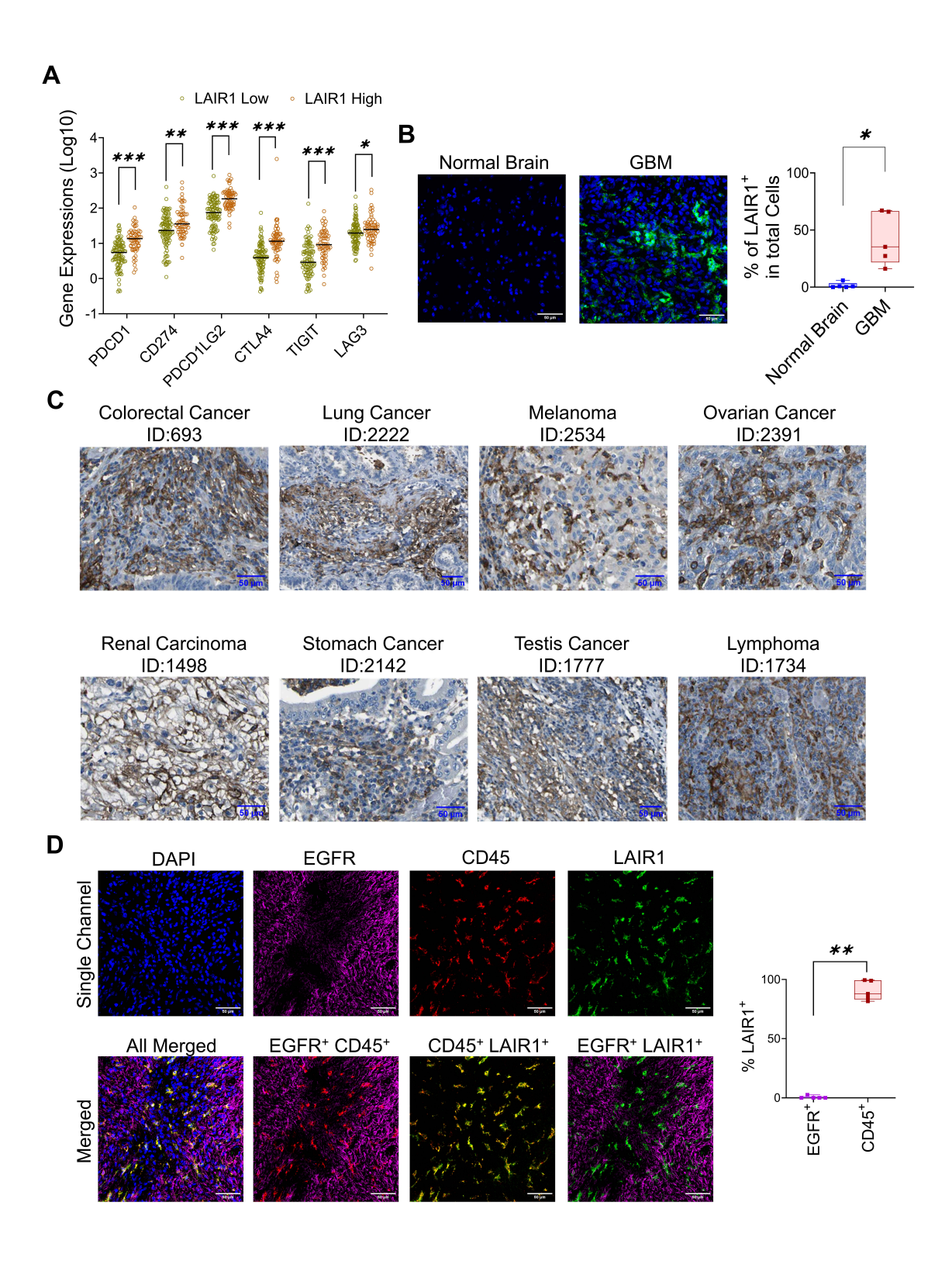
Supplemental Materials for Blocking immune checkpoint LAIR1 with antibody blockade or 3-in-1 CAR T cells enhances antitumor response Haipeng Tao et al. \*Corresponding author. Email: jianping.huang@neurosurgery.ufl.edu This PDF file includes: Supplemental Figures 1 to 15 Legend for Videos 1 to 4 Gating Strategy 1 to 9 Supplemental Methods Supplemental Table 1 Other Supplementary Materials for this manuscript include the following: Videos 1-4 Supporting data values Unedited blot images 



#### Supplemental Figure 1

30

31 32

33

34

35 36

37

38

39

40

41 42

43

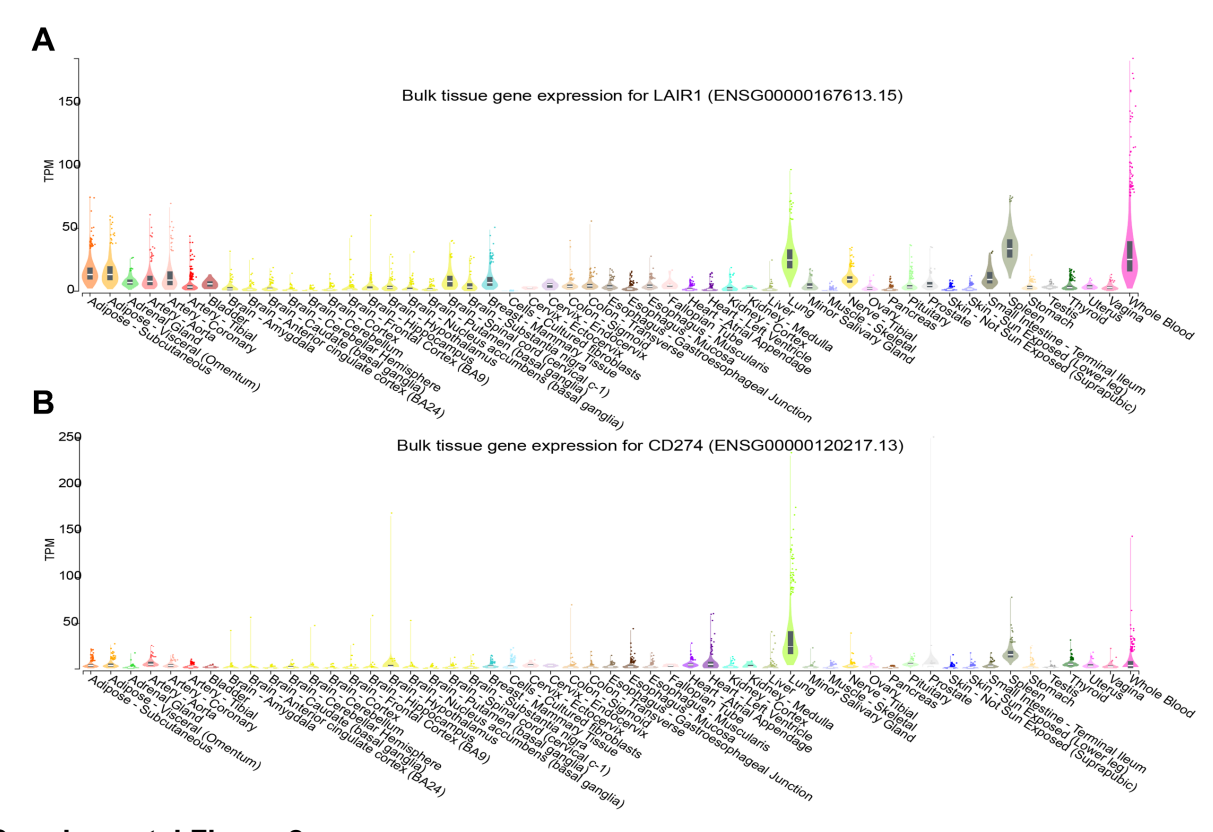
44 45

46

47

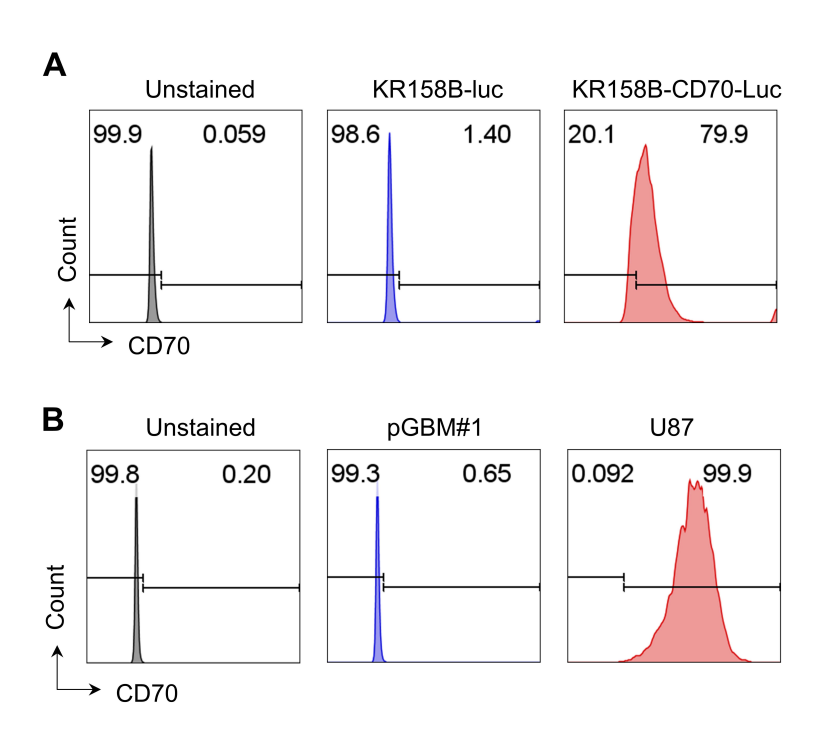
48

LAIR1 expressing cells are present in tumors, and they are on CD45 cells. (A) LAIR1 gene expression is correlated with other immune checkpoints, including PDCD1, CD274, PDCD1LG2, CTLA4, and TIGIT. RNA-seg data were analyzed using the TCGA dataset (n=172). The median value of LAIR1 gene expression was used to separate the LAIR1 high and LAIR1 groups, and the indicated marker expressions [as in log2(x+1) transformed RSEM normalized count] were analyzed. (B) IF staining revealed LAIR1-expressing cells in 5 surgically resected primary GBM tumors (one is shown on the left), and 5 normal brains were utilized as a control. (C) IHC staining revealed LAIR1-expressing cells present in other cancer tissues. The images were acquired from the Human Protein Atlas (https://www.proteinatlas.org/). The origins of each image are documented in the Materials and Methods section. The depicted images are focused on regions containing LAIR1-positive cells. (**D**) LAIR1 expression is predominantly on CD45<sup>+</sup> cells, not tumor cells. IF imaging of one of 5 distinct human GBM samples shows staining with LAIR1, EGFR (tumor marker), and CD45 (immune marker) (left). Quantitative analysis (right) summarizes the percentages of EGFR<sup>†</sup>LAIR1<sup>†</sup> and CD45<sup>†</sup>LAIR1<sup>†</sup> cells. These samples were stained using specific antibodies for CD45, EGFR, and LAIR1, with DAPI used for nuclear staining. Data are represented as Interleaved scatter with median in A, Violin plot with bar in B and D. Statistical significance for the presented findings was determined using the Mann–Whitney U test. \*p < 0.05, \*\*p < 0.01, \*\*\*p < 0.001.

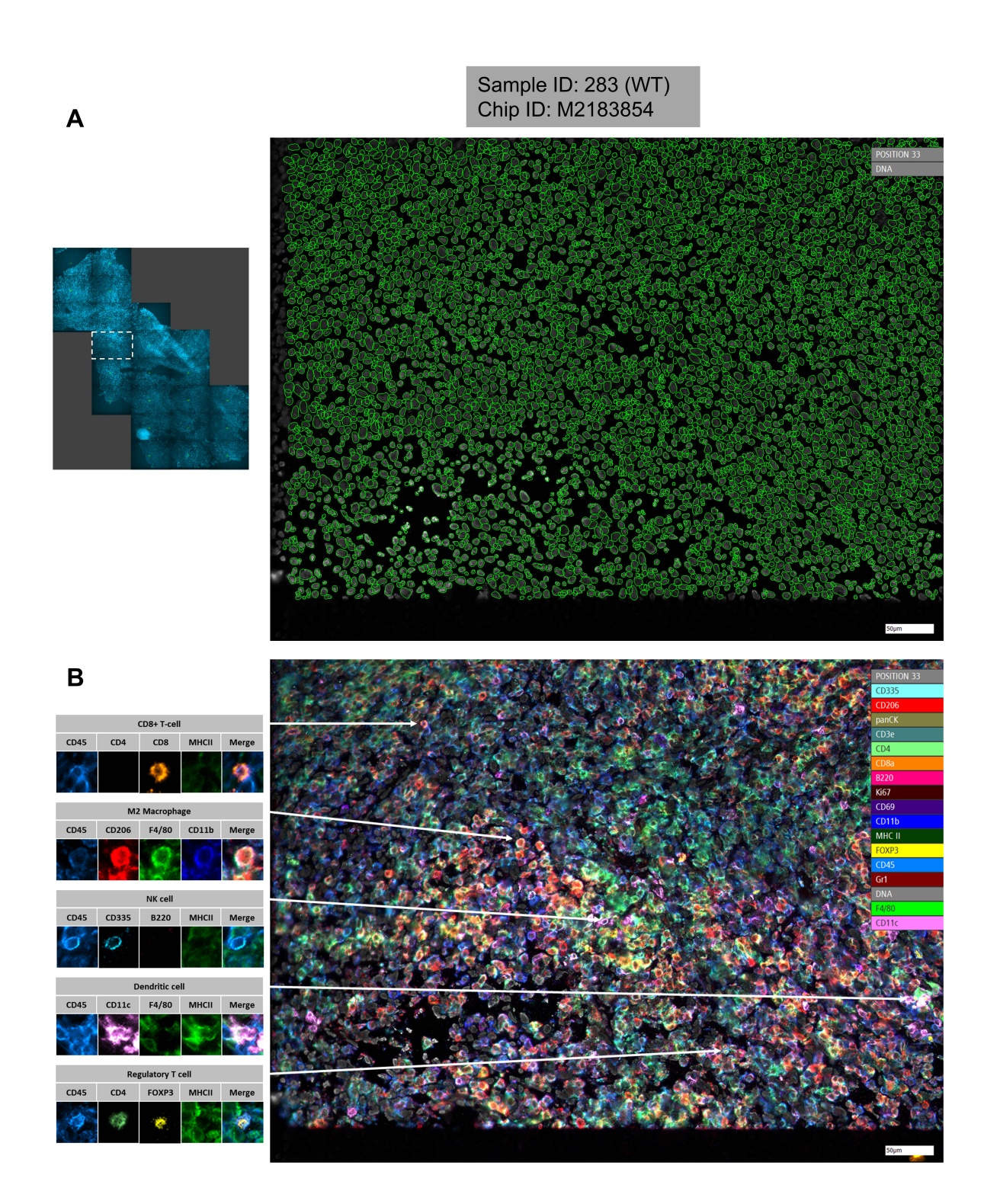


Supplemental Figure 2

Gene expression pattern of LAIR1 on normal tissues is similar to CD274 (PD-L1). Gene expression of LAIR1 (A) and CD274 (PD-L1) (B) in various normal tissues. The data were obtained from the GTEx Portal for LAIR1: <a href="https://gtexportal.org/home/gene/LAIR1">https://gtexportal.org/home/gene/LAIR1</a>, and CD274: <a href="https://gtexportal.org/home/gene/CD274">https://gtexportal.org/home/gene/CD274</a>.



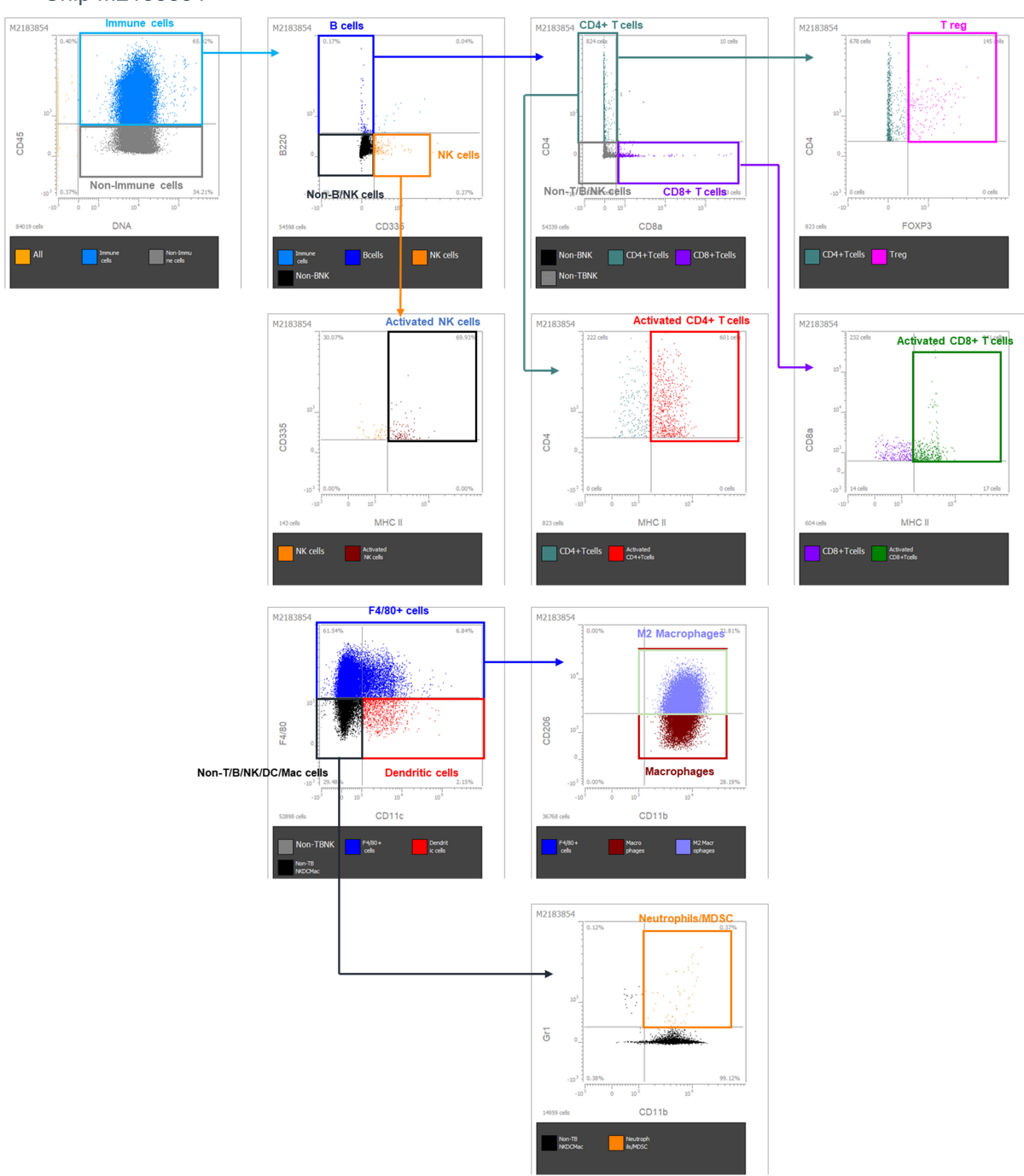
**Supplemental Figure 3 CD70 expression on tumor lines.** (**A**) Flow cytometry (FC) analysis of CD70 expression on murine GBM cell lines KR158B and KR158B-CD70-Luc. (**B**) FC analysis of CD70 expression on human GBM lines pGBM#1 and U87 lines.



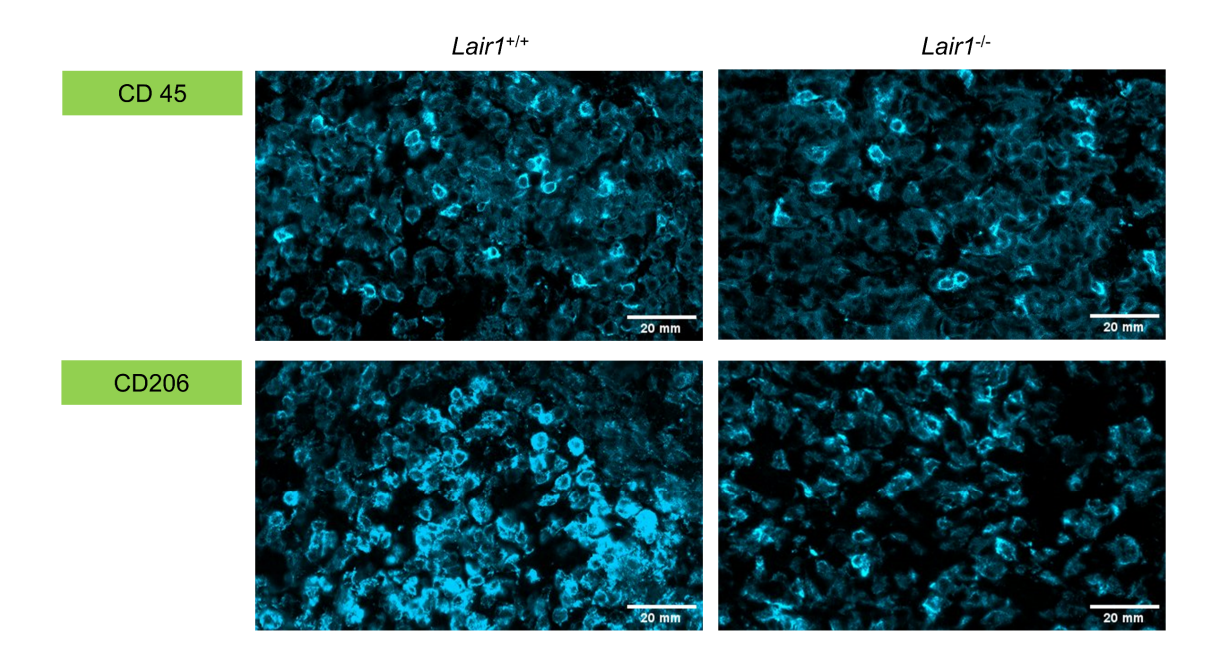
# **Supplemental Figure 4**

Working flow used in **Figure 2H**. (**A**) A rectangular area of the sample was initially scanned, and regions-of-interest (ROI) and tissue integrity were assessed based on auto-fluorescence in prestain QC. Due to the small overall area of the tissue, all areas containing tissue were selected for subsequent scans. DNA stain was used as the basis for automated cell segmentation to identify cells in each sample, allowing cell populations to be identified and quantified. The image shows a DNA stain with segmented cells outlined in green. (**B**) After the selection of ROI based on autofluorescence images, all 17 markers were subsequently stained in cycles. The image to the right shows an overlay of all marker stains in pseudo colors. Fluorescence intensities are automatically calculated for each cell and each marker.

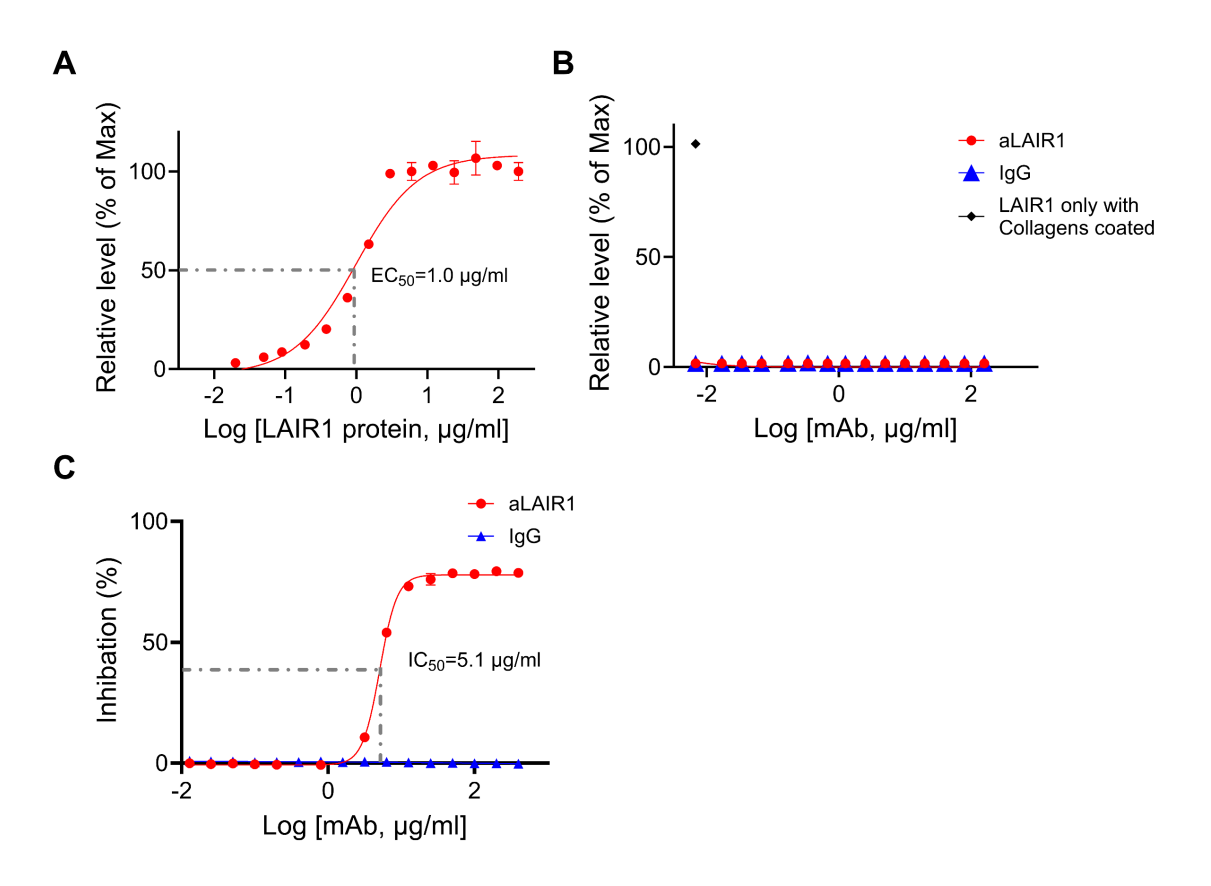
# Sample: 283 Chip M2183854



- 75 Supplemental Figure 5
- 76 The gating strategy in Figure 2H. After automatic segmentation and fluorescence quantification,
- 77 cell type identification was carried out based on a bivariate index-sorting method, which is very
- 78 similar to flow cytometry. Cells are assigned to specific phenotype gates guided based on the
- 79 expression of defining markers. Phenotype population gates are then used as parent gates for
- 80 further sub-phenotyping. This results in a hierarchical gating strategy followed until all desired
- 81 population gates are quantified.
- 82 **B-cells:** CD45<sup>+</sup>B220<sup>+</sup>CD335<sup>-</sup>;
- 83 **NK-cells:** CD45<sup>+</sup>B220<sup>-</sup>CD335<sup>+</sup>;
- 84 **CD4+ T-cells:** CD45<sup>+</sup>B220<sup>-</sup>CD335<sup>-</sup>CD4<sup>+</sup>CD8<sup>-</sup>;
- 85 **CD8+ T-cells:** CD45<sup>+</sup>B220<sup>-</sup>CD335<sup>-</sup>CD4<sup>-</sup>CD8<sup>+</sup>;
- 86 **T-reg:** CD45<sup>+</sup>B220<sup>-</sup>CD335<sup>-</sup>CD4<sup>+</sup>CD8<sup>-</sup>FOXP3<sup>+</sup>;
- 87 Activated CD4 \* T-cells: CD45\*B220\*CD335\*CD4\*CD8\*MHCII\*;
- Activated CD8 \* T-cells: CD45\*B220\*CD335\*CD4\*CD8\*MHCII\*;
- 89 **Dendritic cells:** CD45<sup>+</sup>B220<sup>-</sup>CD335<sup>-</sup>CD4<sup>-</sup>CD8<sup>-</sup>CD11c<sup>+</sup>F4/80<sup>-</sup>;
- 90 Macrophages: CD45<sup>+</sup>B220<sup>-</sup>CD335<sup>-</sup>CD4<sup>-</sup>CD8<sup>-</sup>F4/80<sup>+</sup>CD11b<sup>+</sup>;
- 91 **M2 Macrophages:** CD45<sup>+</sup>B220<sup>-</sup>CD335<sup>-</sup>CD4<sup>-</sup>CD8<sup>-</sup>F4/80<sup>+</sup>CD11b<sup>+</sup>CD206<sup>+</sup>;
- 92 **Neutrophils/MDSCs:** CD45<sup>+</sup>B220<sup>-</sup>CD335<sup>-</sup>CD4<sup>-</sup>CD8<sup>-</sup>CD11c<sup>-</sup>F4/80<sup>-</sup>CD11b<sup>+</sup>Gr1<sup>+</sup>.

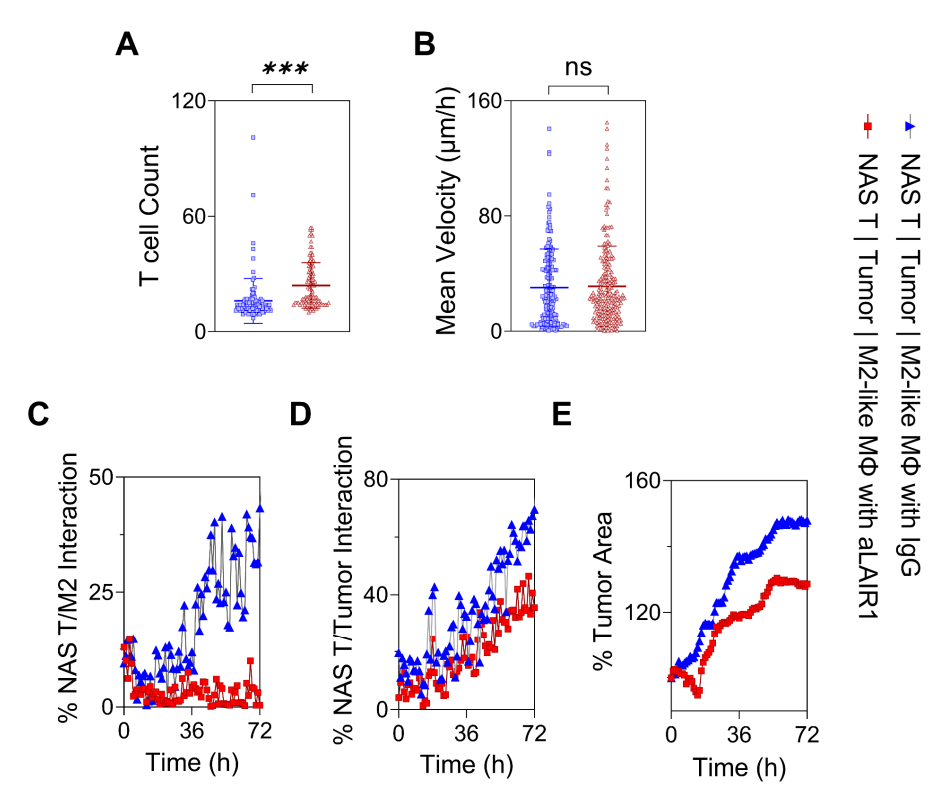


Supplemental Figure 6
Exemplary staining patterns illustrate stain signals from both Lair1\*/- and Lair1\*- and Lair1\*- and Lair1\*- and Lair1\*- and Lair1\*- and Lair1\*- and CD206.



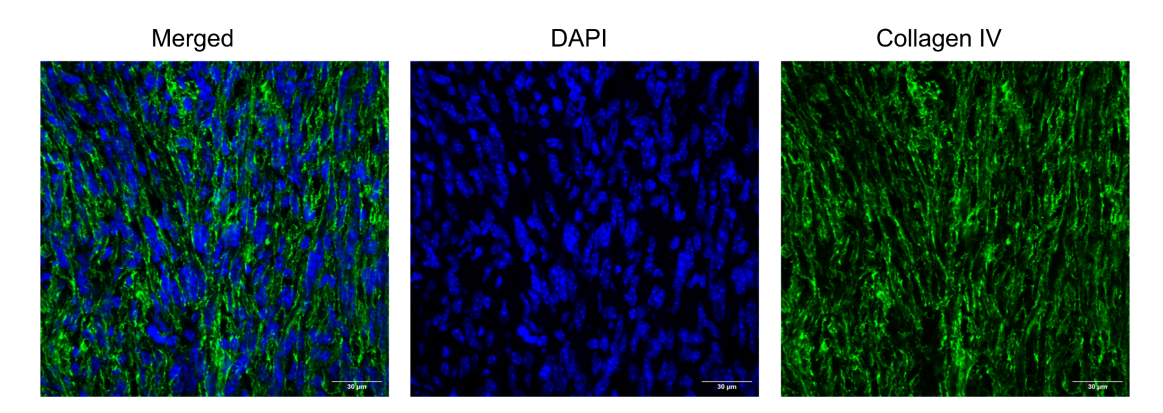
## **Supplemental Figure 7**

Human aLAIR1 inhibits LAIR1-collagen interaction. (A) Soluble human LAIR1-His protein binds specifically to collagens. Increasing concentrations of LAIR1-His were incubated on collagen I/IV—coated plates (10  $\mu$ g/ml) for 2 hours at room temperature. Binding was quantified by His-tag ELISA, confirming the dose-dependent interaction between LAIR1 and collagens. EC<sub>50</sub> was identified. (B) LAIR1-His showed no binding to uncoated plates, confirming its specific interaction with collagen. LAIR1-His (1  $\mu$ g/ml) was pre-incubated with increasing concentrations of human aLAIR1 or IgG for 1 hour, then added to uncoated plates for 2 hours. Three collagen-coated wells served as maximal (Max) binding controls. Binding was quantified by His-tag ELISA and reported as % response relative to the LAIR1-only collagen-coated control. (C) aLAIR1 effectively inhibits LAIR1-collagen binding in a dose-dependent manner. Pre-incubation of LAIR1-His with aLAIR1 or IgG was performed as described in B, followed by incubation on collagen I/IV-coated plates for 2 hours at room temperature. Binding was quantified by His-tag ELISA. The % of inhibition was calculated as: 1 – (% of the relative level). All experiments were independently repeated at least twice. Data are presented as mean ± SD. The IC<sub>50</sub> value was calculated by nonlinear regression using a four-parameter logistic model.

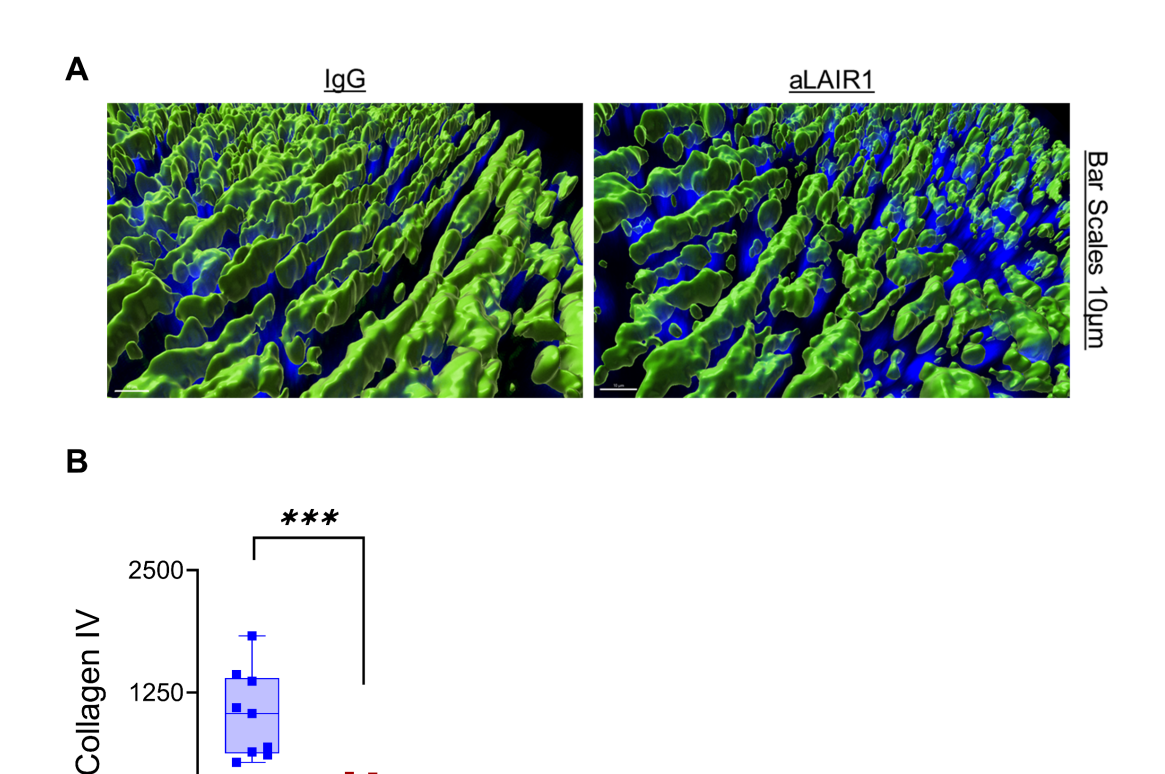


**Supplemental Figure 8** 

Impact of aLAIR1 on Non-Antigen Specific (NAS) T cells in the presence of M2-like M $\Phi$  within the 3D printing system (The experimental design is shown in Figure 3D, and the data were calculated from Vides 1, C and D). (A and B) The total number or the mean velocity of NAS T cells in the presence of IgG or aLAIR1. (C and D) The kinetic change in % of NAS T Cell/Tumor interaction in the presence of IgG or aLAIR1. The parameter was measured by the overlapped region of NAS T/ tumor or CAR T/tumor signals as a percent of total T cells. (E) No impact on tumor inhibition for IgG and aLAIR1. The tumor area was measured as a percent of the original tumor mass. Data are represented as Mean  $\pm$  SD in A and B; Points and connecting lines in C-E. Statistical significance for the presented findings was determined using the two-sample t-test in A and B. Generalized estimating equation (GEE) models in (C and E, p< 0.001, between IgG and aLAIR1). \*\*\*p< 0.001



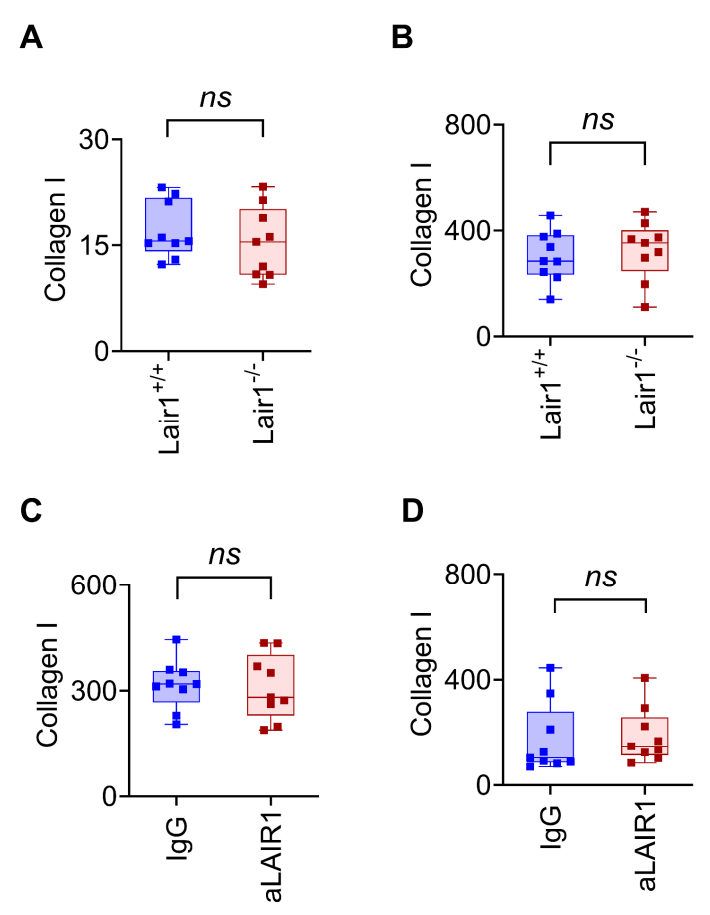
Supplemental Figure 9
A Representative image of collagen IV in the 2D model. Collagen IV expressions in tumor from Figure 6C before 3D reconstruction. Collagen IV (green) structure and DAPI (blue) for nuclei staining.



**Supplemental Figure 10** 

<u>lgG</u>

**Collagen IV expression in IgG and aLAIR1 treated GBM model.** (**A** and **B**) Nine tumor tissue sections collected from 3  $Lair1^{*/+}$  KR158B-CD70-Luc GBM TB-mice 63 days post-treatment, respectively, described in **Figure 4A**, were stained with IF for collagen IV (green) and DAPI (blue) nuclei staining. The comparison of collagen IV fibers in relationship with tumor nuclei for the aLAIR1 and IgG control groups from representative images and quantitative comparisons are shown. Data are represented as a violin plot in **B**. Statistical significance for the presented findings was determined using the GEE model. \*\*\*p < 0.001.



**Supplemental Figure 11** 

**LAIR1 inhibitions do not alter collagen I in normal brains and tumors.** aLAIR1 doesn't impact collagen I expressions. The fluorescent intensity of collagen I in normal brains and tumors (n=9) was measured by IF. (**A-E**) Comparison of collagen I in normal brains using the same tissues in **Figure 6A** and tumors used in **Figure 6C** (GBM, *Lair1*<sup>-/-</sup>) and **E** (LLC1, aLAIR1 treatment), and **Supplemental Figure 10** (GBM, aLAIR treatment). The expression of collagen I was measured by MFI. Data are represented as violin plots. Statistical significance for the presented findings was determined using the GEE model. *ns:* Not significant.

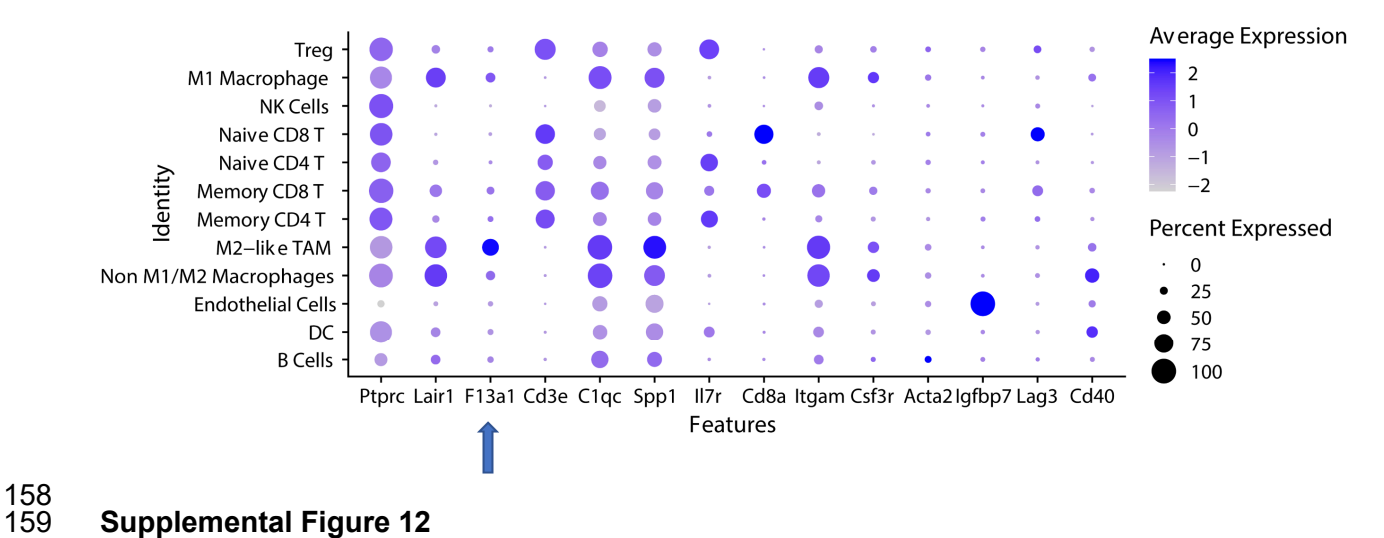
161

162 163

164

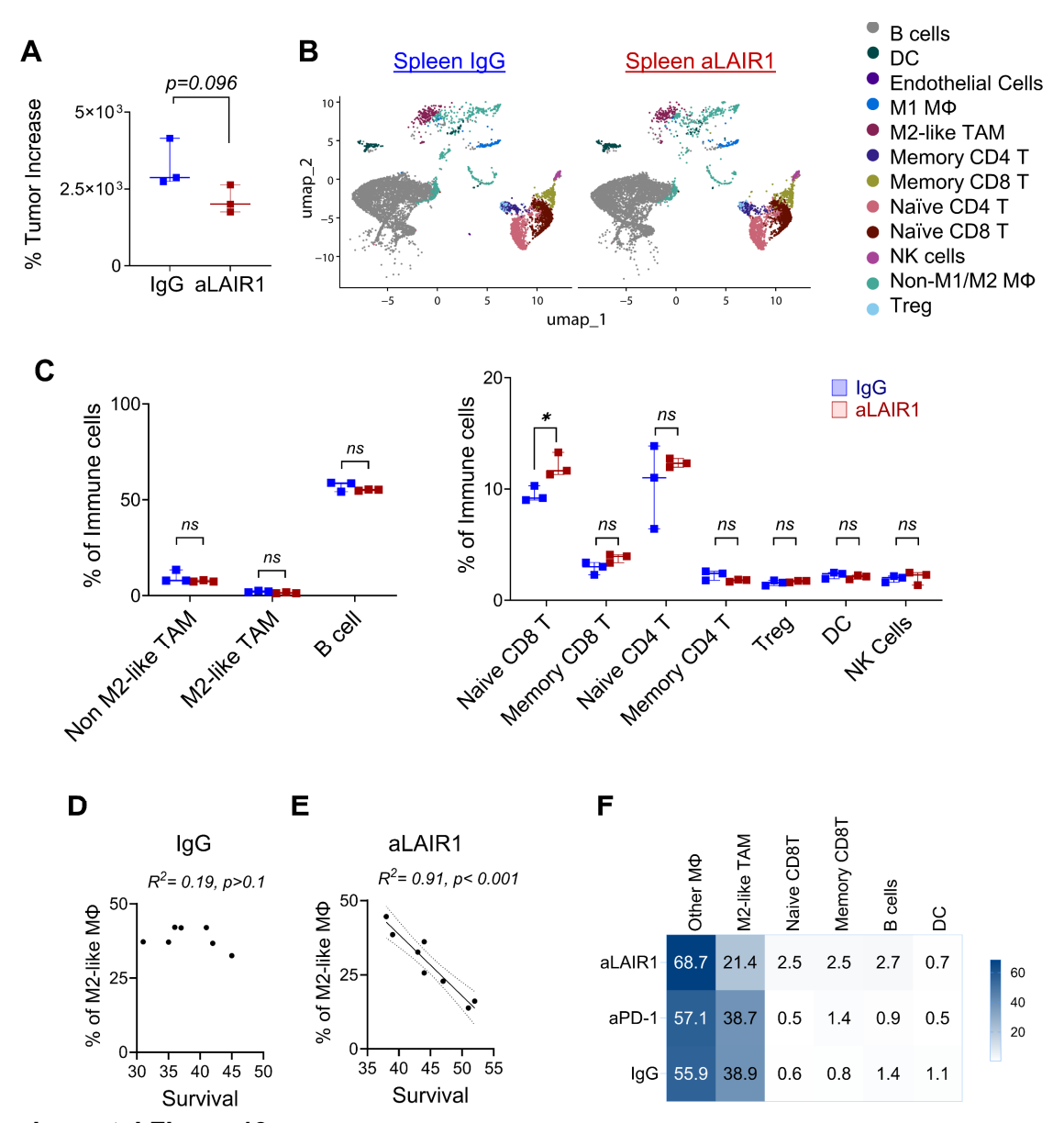
165

166



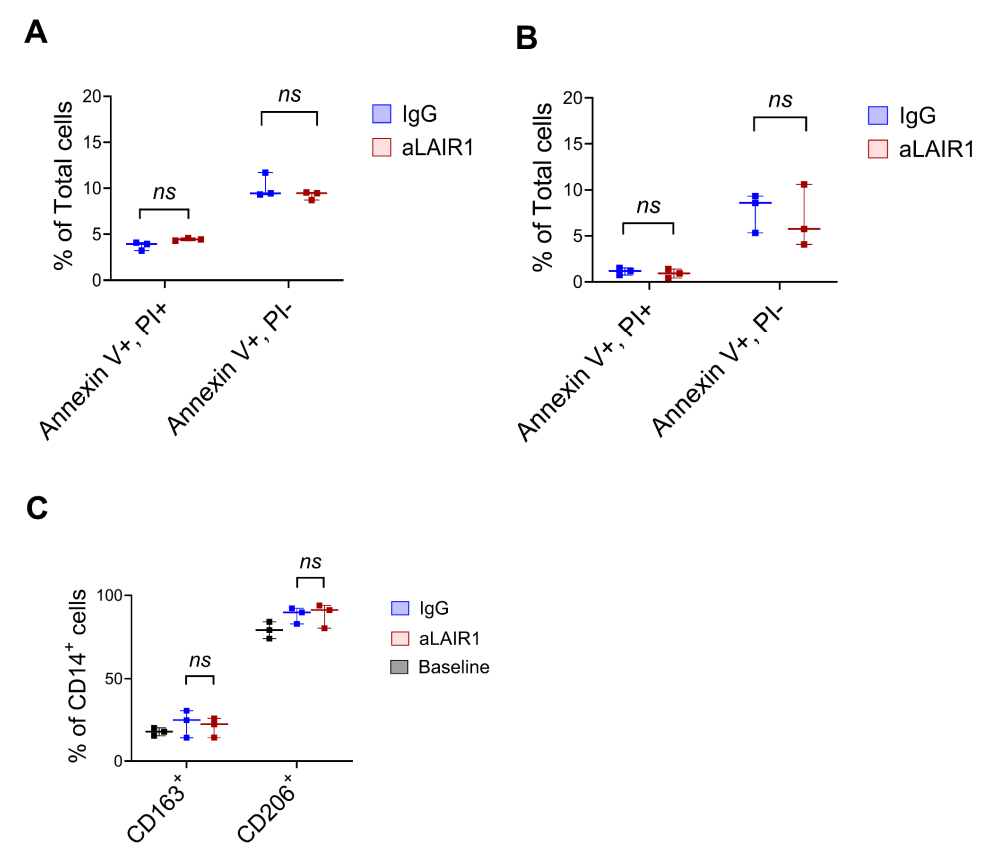
# **Supplemental Figure 12**

Cell population identification and signature gene expressions. The dot plot defined the cell populations in scRNA seq described in Figure 6, G-J and Supplemental Figure 13 B, C, and F. The Y-axis depicts the names of the cell types; the X-axis depicts the gene identity. Expression is noted according to the number of cells that express the marker above the background (the diameter of the circle increases with the fraction of cells expressing the marker); The average intensity is represented by a color gradient varying from white (no expression) to purple (midintensity expression) and to blue (maximum expression). The F13a1 is indicated by the blue arrow.



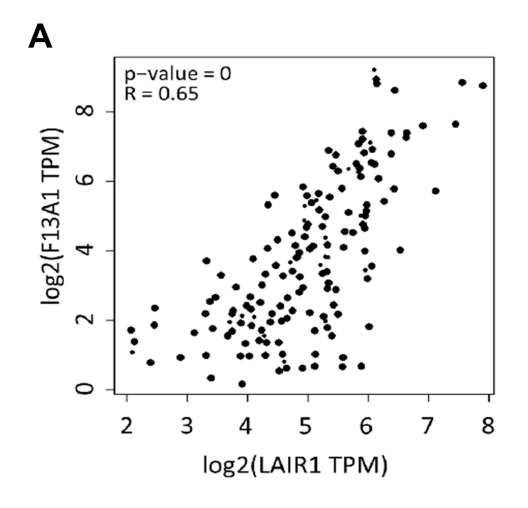
Supplemental Figure 13

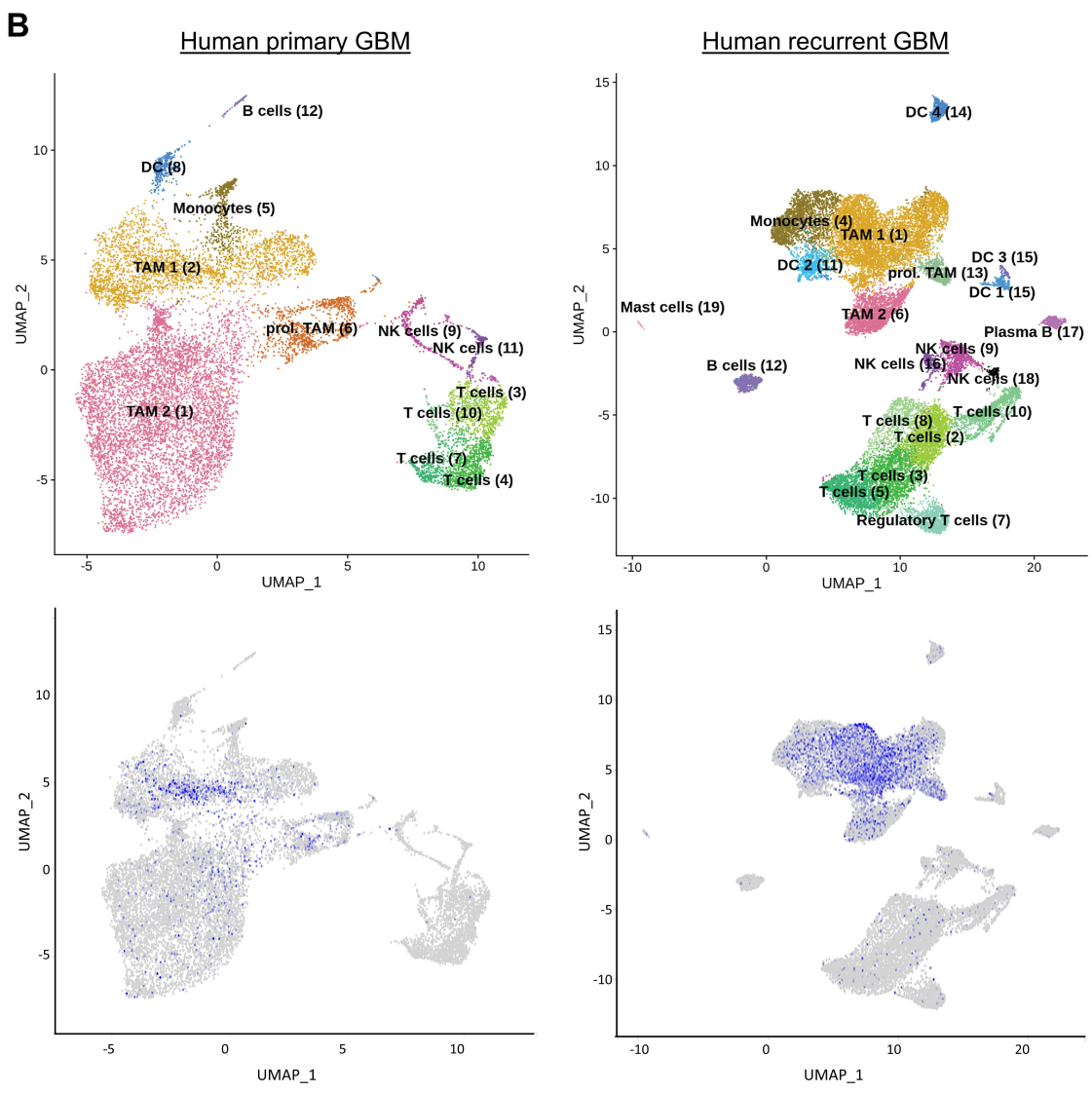
aLAIR1 modulates immune cells in peripheral tissues and tumors. (A) C57BL/6 TB-mice (KR158B-CD70-Luc, 3/group) received IgG or aLAIR1 treatment (Figure 4A). Tumor increase after the treatment was calculated 48 days post-treatment using IVIS signals related to the baseline (day -7). (B-C) The tumor (Figure 6G-H) and spleen tissues were analyzed by scRNA-seq 49 days after treatment. UMAPs illustrate immune cell clusters from spleens (B), with population summaries (>1%) shown in C. (D-E) Female C57BL/6 mice (8/group) were implanted i.c. with KR158B-Luc (1×10<sup>4</sup> cells/mouse) and treated with 5 doses of aLAIR1 or IgG (200 µg/dose, i.p., every other day from day 0 to 8). Survival was monitored, and tumors were harvested at the endpoint. M2-like TAM frequencies were quantified by FC and correlated with survival by regression analysis. (F) The same tumor model as in (D-E) was treated with IgG, aLAIR1, or aPD-1 (200 µg/dose, 3/group, 5 doses every other day). Tumors were collected on day 28, and pooled cells from each group were analyzed by scRNA-seq. Cell populations >1% are summarized. Data are represented as Box-and-whiskers plots (A and C). Statistical significance was determined using two-sample t-tests (A and C), and Pearson analysis (D-E). ns: Not significant, \* p < 0.05.



**Supplemental Figure 14** 

**aLAIR1 does not influence the apoptosis and phenotyping of LAIR1-expressing cells. (A** and **B**) The apoptosis of LAIR1-expressing cells (n=3) was not impacted by aLAIR1. Human THP-1 cells (a LAIR1-expressing human monocyte line) and human PBMC-induced M2-like M $\Phi$  were treated daily with 5 µg/ml of IgG or aLAIR1 for 3 days; the viability of these cells was assessed by flow cytometry using Annexin V and Propidium Iodide (PI). Annexin V PI cells represent early apoptosis cells and Annexin V TPI cells are late apoptosis cells. (**C**) The phenotyping of M2-like M $\Phi$  in **B** was assessed by flow cytometry using CD163 and CD206. Data are represented as violin plots. A two-sample t-test was used to compare. FDR correction was applied in **C**. *ns*: Not-significant





# **Supplemental Figure 15**

F13a1 expression in GBM patients. (A) Regression analysis between F13a1 and LAIR1 gene expressions in GBM was analyzed using the Pearson correlation coefficient from the TCGA database(<a href="http://gepia.cancer-pku.cn/detail.php?gene=lair1">http://gepia.cancer-pku.cn/detail.php?gene=lair1</a>). (B) The UMAP of F13a1 expressing cells represents TAM (M2-like MΦ) in primary (left) and recurrent (right) GBM using the Brain Immune Atlas database (https://www. brainimmuneatlas.org/index.php).

# 202 Legend for Videos 1-4

Real-Time Monitoring of aLAIR1 Reversing M2-Like Macrophage-Mediated Inhibition of CAR T Cells in a 3D Model. Both 8R-CD70CAR T cells and Non-Antigen Specific (NAS) T cells, as well as M2-like MΦ, were derived from the same human PBMC. The labeled M2-like MΦ (green) and 8R-70CAR T or NAS T cells (red) were co-cultured with the CD70<sup>+</sup>U87 GBM line (blue-white) (cell ratio=5:1:2.5). Cultures were treated daily with either IgG or aLAIR1 (5 μg/ml/day) over 105 hours.

208 209

The experimental conditions were as follows:

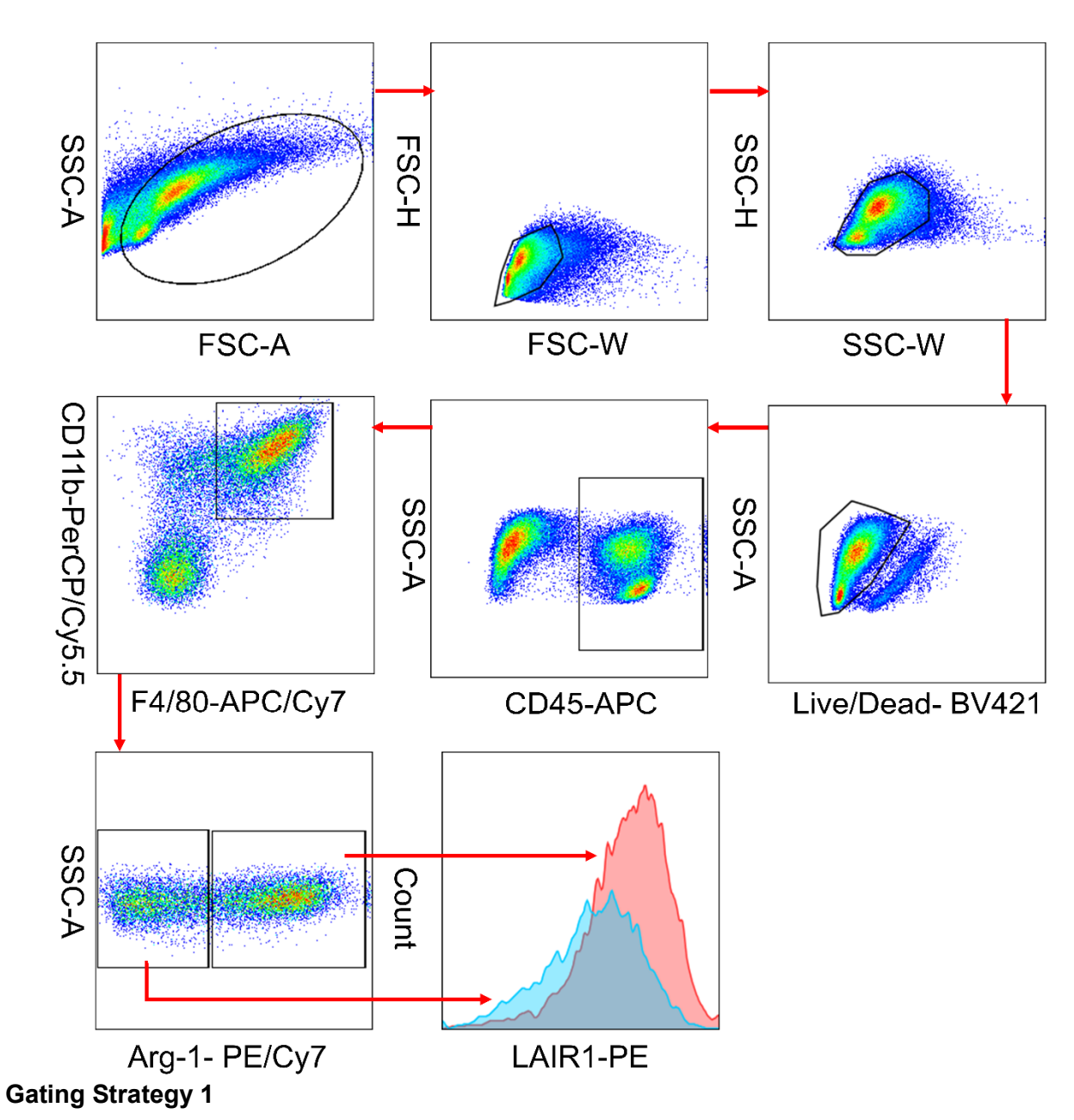
- 210 (A) 1. 8R-70CAR T cells + M2-like MΦ + Tumors + aLAIR1
  - 2. 8R-70CAR T cells + M2-like MΦ + Tumors + IgG
  - 3. NAS T cells + M2-like MΦ + Tumors + aLAIR1
  - 4. NAS T cells + M2-like MΦ + Tumors + IgG

213214215

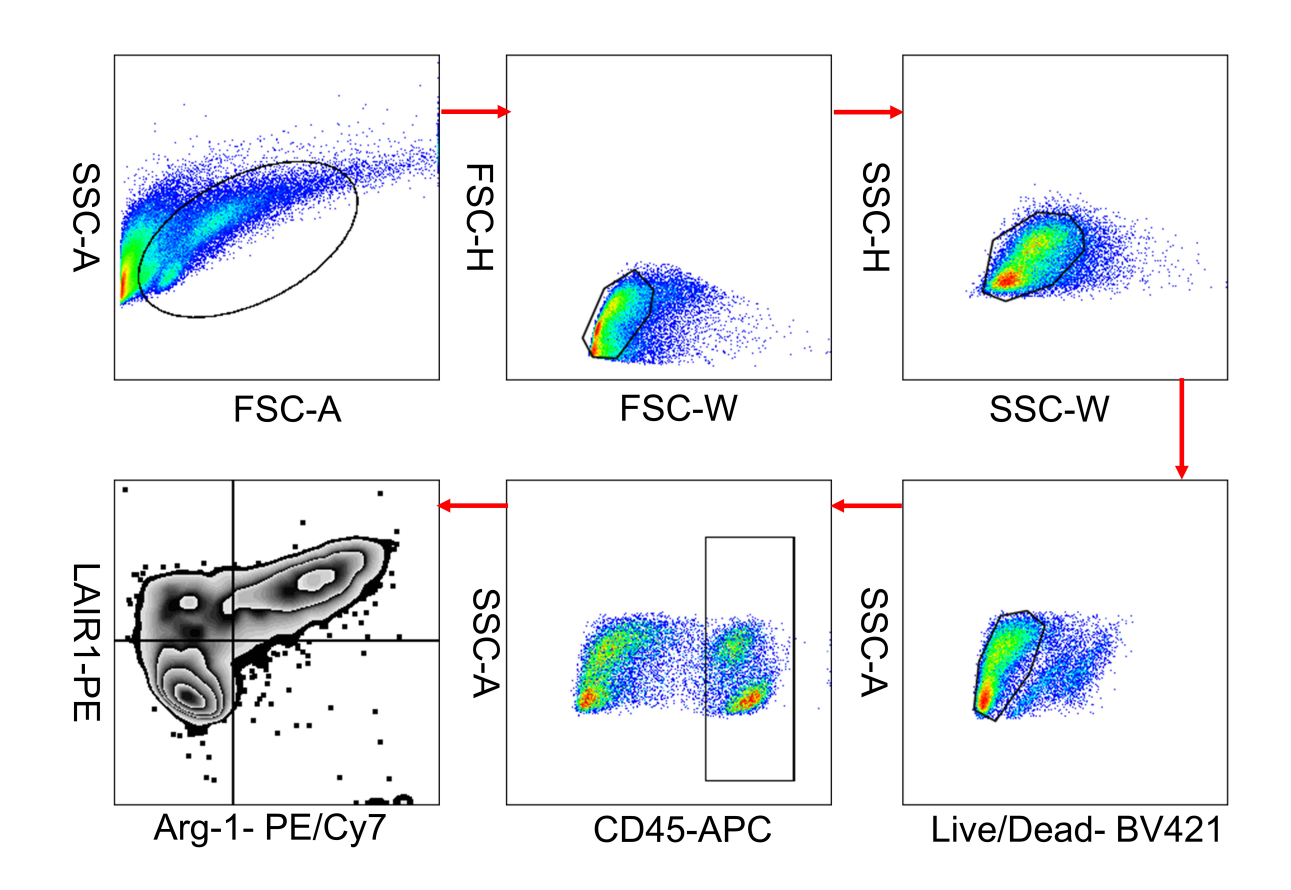
211

212

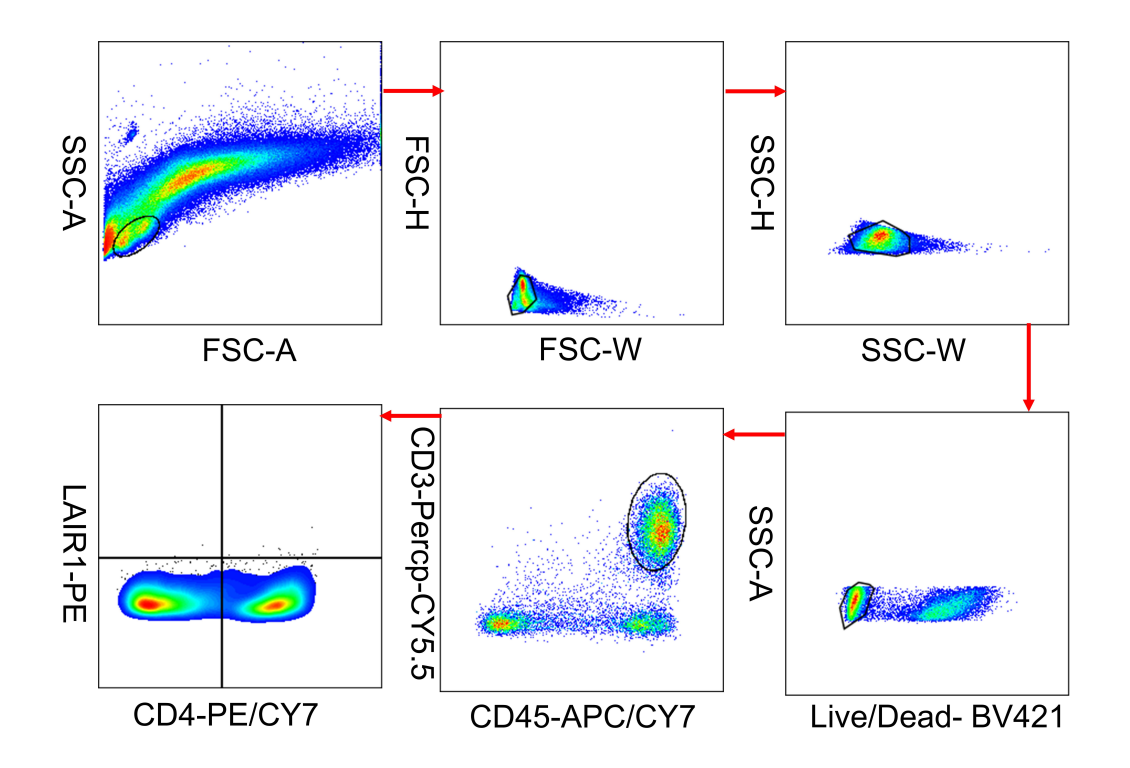
Quantitative results are presented in Figure 3G-K and Supplemental Figure 8A-E.



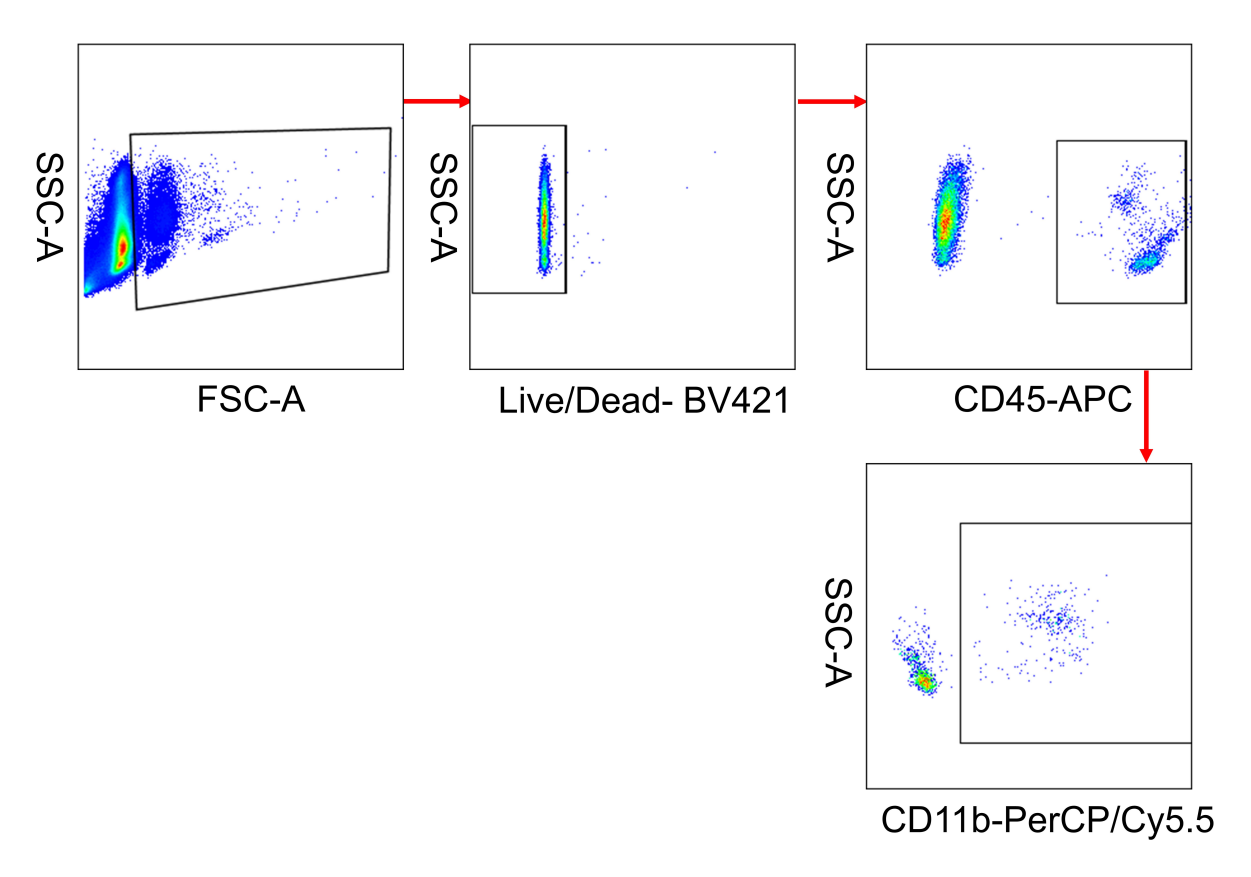
**Gating strategy for Figure 1**, **F** and **G**. Detection of the relative % of Arg-1<sup>+</sup> M2-like TAM in the total CD45<sup>+</sup> cells in **Figure 1F** and MFI of LAIR1 in M2-like TMA and Mon M2-like TAM depicted in **Figure 1G**.



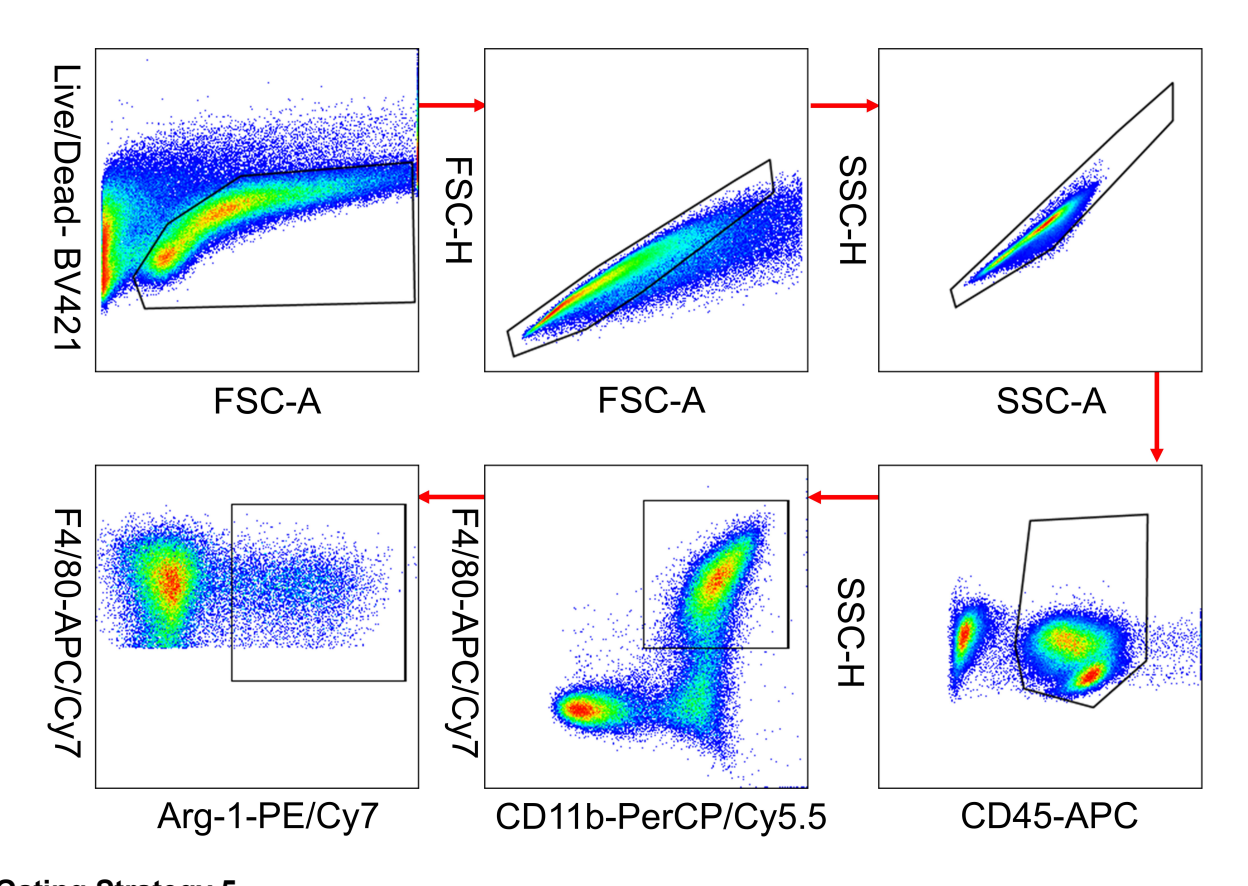
Gating Strategy 2
Gating strategy for Figure 1 H left. Detection of the LAIR1 expression on Arg-1 M2-like TAMs.



Gating Strategy 3
Gating strategy for Figure 1 H right. Detection of the LAIR1 expression on T cells.

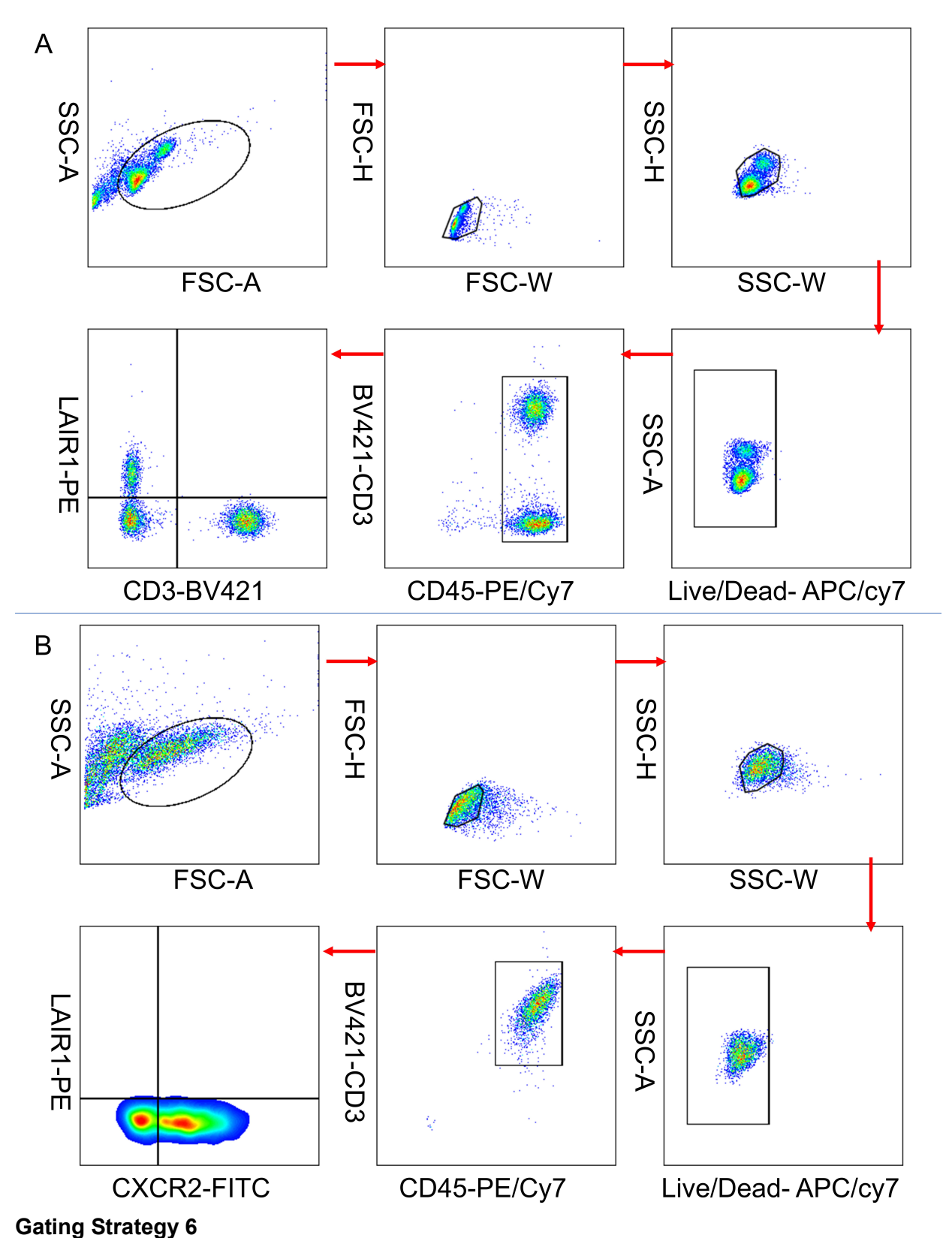


**Gating Strategy 4 Gating strategy for Figure 2C.** Detection % of CD45<sup>+</sup>CD11b<sup>+</sup> myeloid cells in peripheral blood between *Lair1*<sup>+/+</sup> and *Lair1*<sup>-/-</sup> mice.

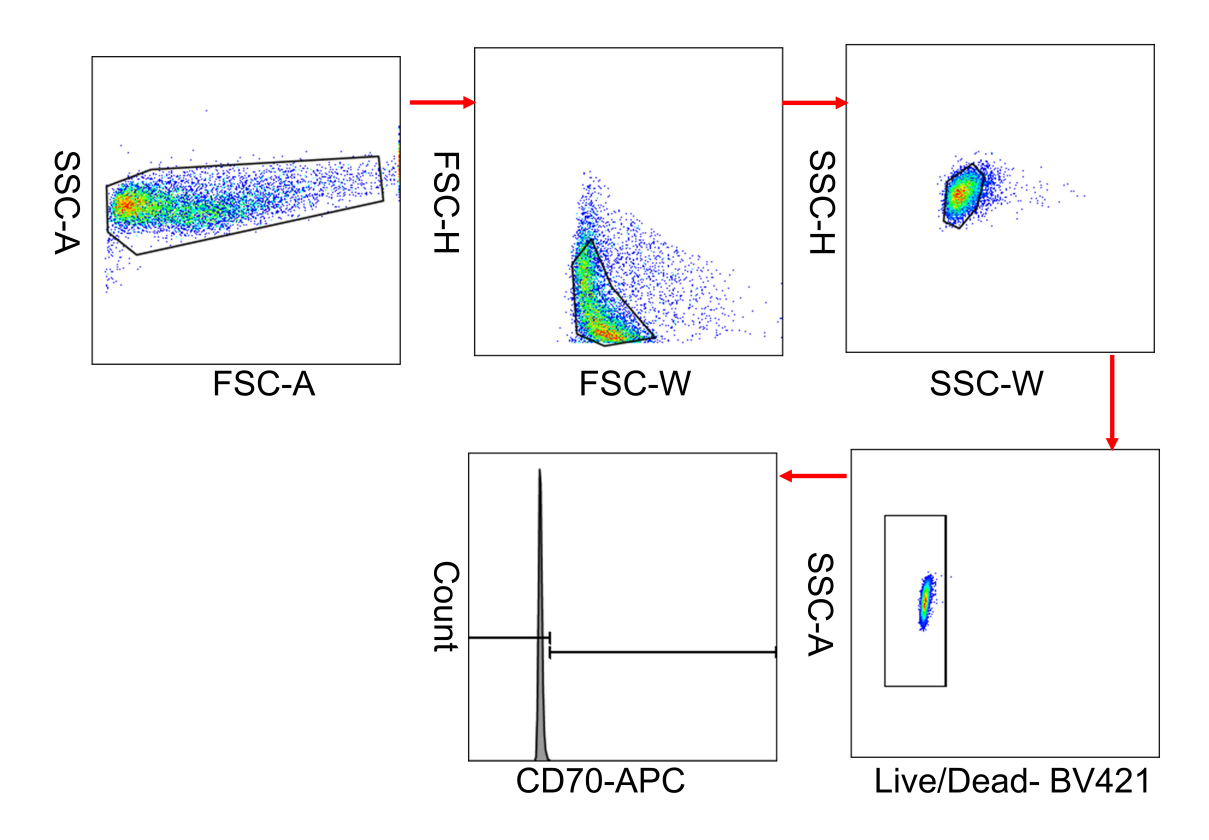


Gating Strategy 5

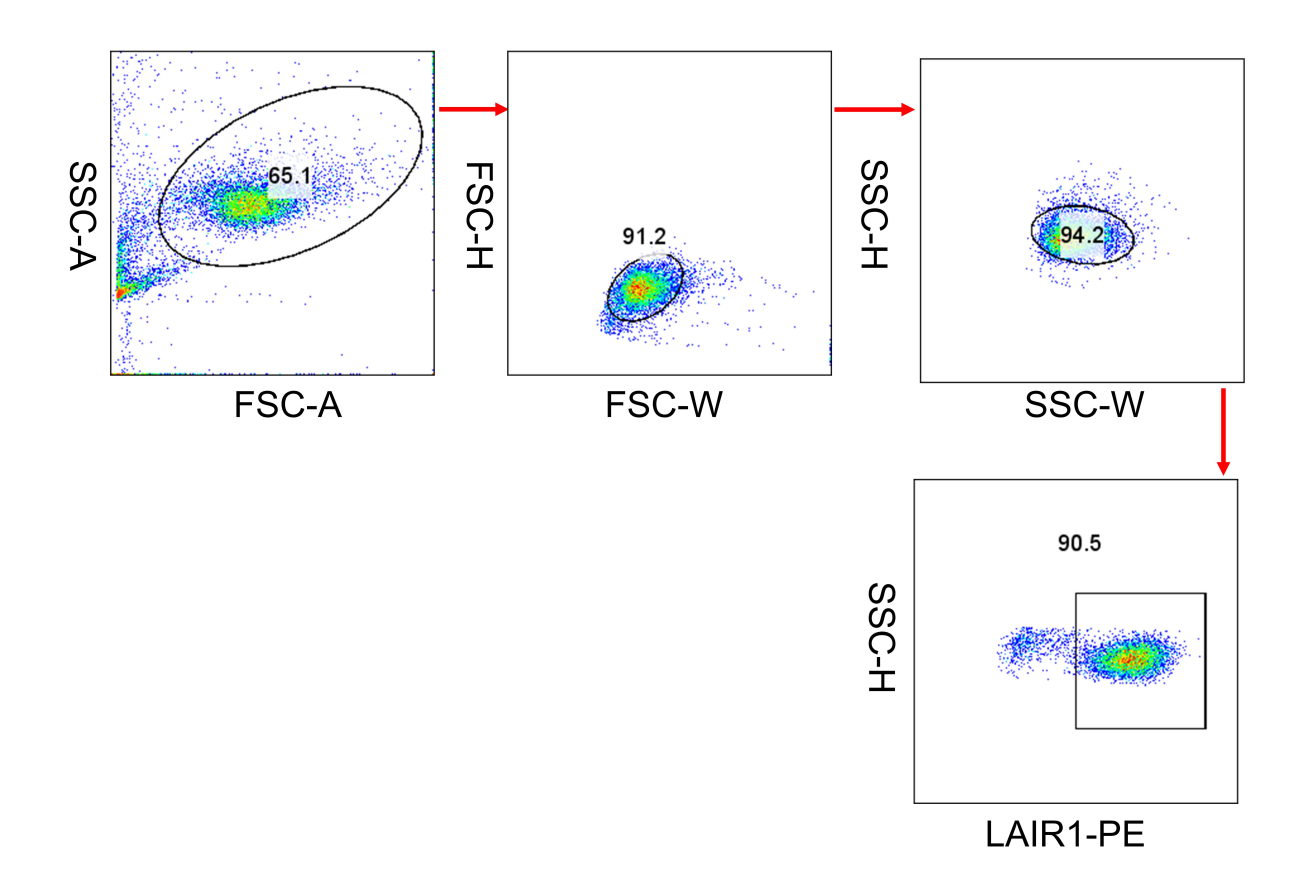
Gating strategy for Figure 2G and Figure 6F. Detection of MΦs, identified as % of CD45<sup>+</sup>CD11b<sup>+</sup> F4/80<sup>+</sup>, and M2-like TAM, identified as % of CD45<sup>+</sup>CD11b<sup>+</sup> F4/80<sup>+</sup>Arg-1<sup>+</sup> using tumors from *Lair1*-/- mice.

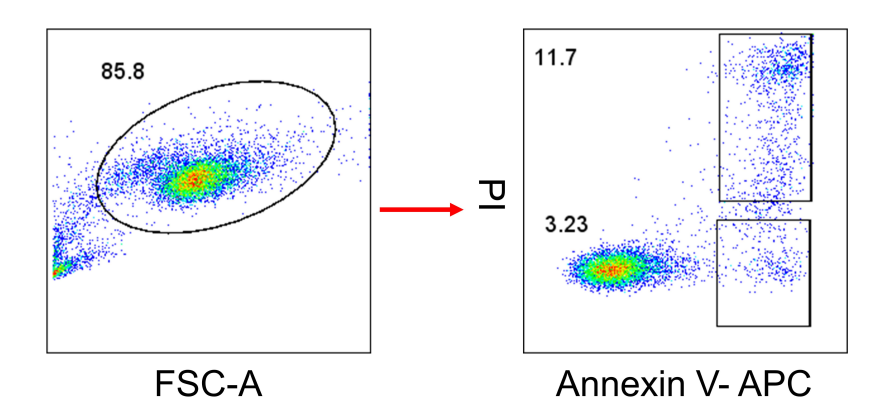


**Gating strategy 6 Gating strategy for Figure 3D.** Detection of LAIR1 expression on PBMC (**A**) and 8R-70CAR T cells (**B**).

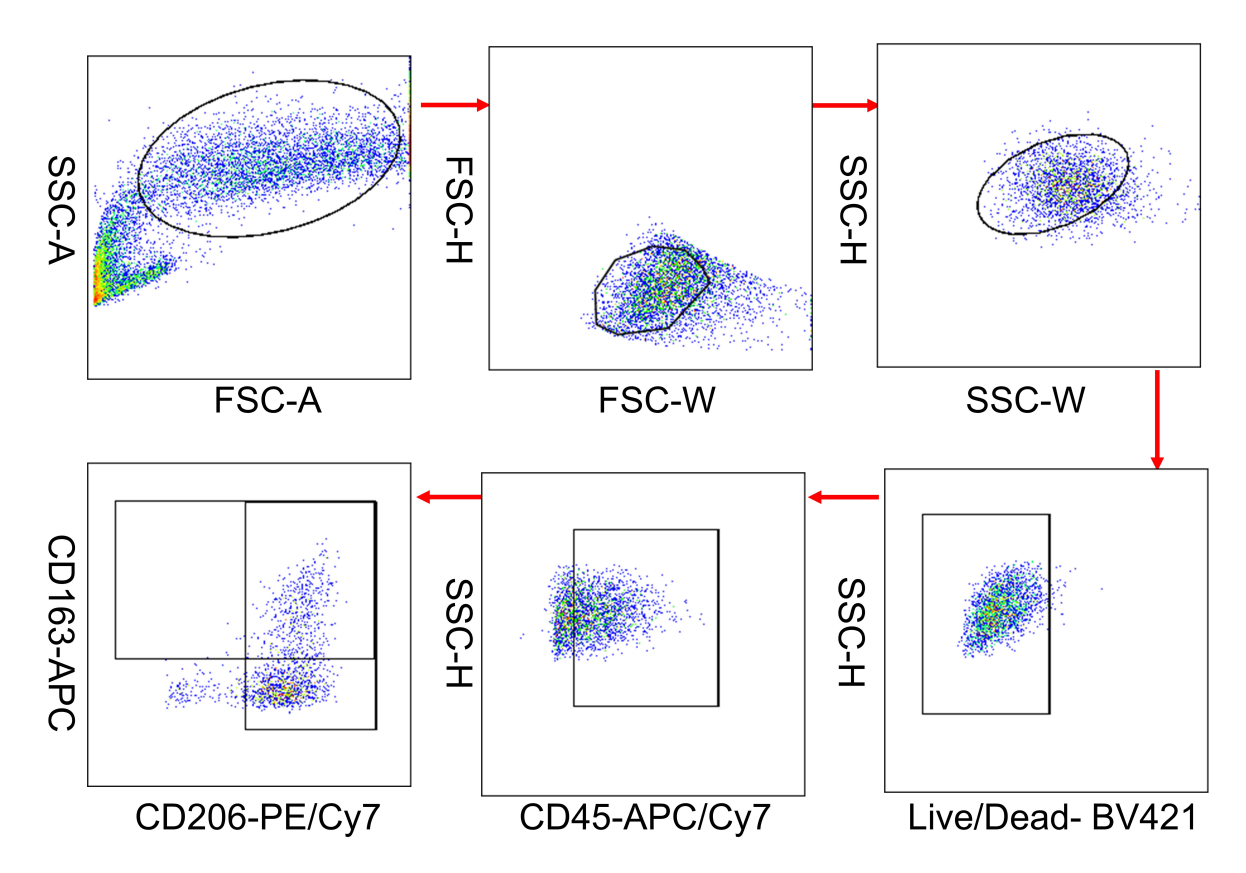


Gating Strategy 7
Gating strategy for Supplemental Figure 3. Detection of CD70 expression on tumor lines





Gating Strategy 8 Gating strategy for Supplemental Figure 14, A and B. Detection of LAIR1 expression on Thp-1 and PBMC induced M2-like M $\Phi$  (Upper), and apoptosis of cells treated by IgG or aLAIR1 (Downer).



Gating Strategy 9 Gating strategy for Supplemental Figure 14C. Detection of Phenotyping of M2-like M $\Phi$  Treated with aLAIR1 or IgG Control

## **Supplemental Methods**

#### Cell Culture

Murine GBM lines KR158B, KR158B-Luciferase (Luc), KR158B-CD70-Luc, GL261-Luc, or Human GBM line U87 was cultured in Dulbecco's Modified Eagle Medium (DMEM, Thermo Fisher Scientific, 11965092) with 10% Fetal Bovine Serum (FBS, Avantor, 89510) and 1% Penicillin-Streptomycin (Thermo Fisher Scientific,15140163) without sodium pyruvate. The Murine Lewis lung carcinoma line (LLC1) was cultured using Dulbecco's Modified Eagle Medium F12 (DMEM/F12, Thermo Fisher Scientific, 12634028) supplemented with 10% Fetal FBS and 1% Penicillin-Streptomycin. THP-1 line was cultured with RPMI 1640 media with 10% Fetal FBS and 1% Penicillin-Streptomycin. GP2-293 and 293T/17 cells were cultured in DMEM with 10% FBS and 1% Penicillin-Streptomycin containing sodium pyruvate. Human T cells were cultured with AIM-V media (Thermo Fisher Scientific, 087-0112DK) containing 100 IU/mI IL-2 (R&D systems, 202-IL-500) with 5% Human AB serum (Fisher Scientific, HP1022HI)(1). Human Monocytes/MΦs were cultured with AIM-V media with 5% Human AB serum. Cells were kept in 37°C incubators with 5% CO2.

### **Cell Isolations**

1. Human PBMC and peripheral blood lymphocytes (PBL) isolations: PBMC were isolated from Buffy Coats of healthy donors (LifeSouth Community Blood Centers, Gainesville, FL) using density gradient centrifugation method. Briefly, the blood was diluted in PBS followed by Histopaque-1077 (Sigma-Aldrich, H8889-500ML) spin down for 400 x g, 30 min at room temperature. Then, the red blood cells (RBC) were removed by 10X RBC Lysis Buffer (Thermo Fisher Scientific, 00-4300-54), incubating for 3 min in a water bath. The PBL were isolated by plating the PBMC for 2 hours within AIM-V media plus 5% Human AB serum. The non-adherent cells were collected and stored at liquate nitrogen

- 2. <u>Mouse T cell isolation</u>: Healthy C57/B6 mice spleens were utilized to isolate murine T cells. Splenocytes were obtained by mashing the spleen with a cell strainer (Fisher Scientific, 08-771-2) and removing red blood cells using a 10X RBC Lysis Buffer. Mouse peripheral blood was collected through the fiscal vein, 50-100µl per mouse. The isolation of T cells was carried out using the Pan T kit from Miltenyi Biotec (130-095-130). Subsequently, the T cells were cultured in RPMI 1640 media (11-875-119) supplemented with 30IU/ml human IL-2, 10% FBS, 1% Non-Essential Amino Acids (NEAA, 11-140-050), 1% Sodium Pyruvate (11-360-070), 1% antibiotic-antimycotic (15240062), 0.1% 2-Mercaproethanol (21-985-023), and 1% L-Glutamine (25030-164) sourced from Thermo Fisher Scientific.
- 3. Mouse tumor single cell suspension: To prepare a single-cell suspension from tumor tissue, we used an enzymatic digestion protocol based on the 'Triple Enzyme Mouse Tumor Digestion' method provided by the NCI. Briefly, the tumor tissues were resected and digested with 1mg/ml Collagenase (C5138), 20 Units/ml DNase (D5025), and 0.1 mg/ml Hyaluronidase (H6254) from Millipore Sigma in gentleMACS™ Octo Dissociator (Miltenyi Biotec) for getting single-cell suspension.

### 4. Mouse bone marrow isolation

Bone Marrow Isolation Using the Flushing Method. Cut open both ends of the bone to expose the bone marrow; Fill a 10 mL syringe with 10 mL ice-cold RPMI 1640 medium and attach to a 21-gauge needle; Flush out the bone marrow into a centrifuge tube(2). Then, the RBCs were removed by 10X RBC Lysis Buffer, incubating for 3 min in a water bath.

#### **CAR T Cells Transduction**

303

304 The human or mouse T cells were transduced with either human control vector (pMSGV8, Ctrl), 305 8R-70CAR, L2-8R-70CAR, or mouse CD70CAR, and the transduction efficiency was determined 306 as described previously (1, 3). Briefly, CD70CAR with different modifications was generated via 307 transfection of GP2-293 cells. For retrovirus production, GP2-293 cells were transfected 308 with 2 µg of pMD2.G (Addgene 12259) and 2 µg of described CAR plasmid using 10 µl of 309 Lipofectamine 2000 (Thermo Fisher Scientific, 11668019) in 700 µl of OPTI-MEM (Thermo Fisher 310 Scientific, 31985070). The supernatants were collected 48 hours post-transfection following the 311 CAR transduction procedure. 312 Human T cells, isolated from PBMCs, were activated 72 hours prior to transduction using anti-313 CD3/anti-CD28 Dynabeads (Thermo Fisher Scientific, 11161D) at a cell-to-bead ratio of 1:1. 314 Mouse T cells were isolated from splenocytes using the Pan T Cell Isolation Kit, and activated for 315 48 hours on plates coated with anti-CD3 (Biolegend, 100340, 1 µg/ml) and anti-CD28 (Biolegend, 316 102116, 2 µg/ml) antibodies. To facilitate transduction, non-tissue culture-treated plates were 317 coated with 20 µg/ml of RetroNectin (Clontech Laboratories, T100A). The CAR T cells were used 318 72 hours post-transduction.

#### M2-like MΦ Generation

319

320

321

322

323

324

325

1. Human CD14<sup>+</sup> cells were isolated from human PBMC by CD14<sup>+</sup> positive selection beads (Miltenyi Biotec, 130-050-201), then treated with 20 ng/ml M-CSF (PeproTech, AF-300-25) for 5 days, and then cells were then spiked with 20 ng/ml M-CSF, IL-4 (AF-200-04), IL-6 (AF-200-06), IL-13 (AF-200) from PeproTech, and 20 ng/ml IL-10 (R&D Systems, 217-IL-010) for an additional 4 days in AlM-V media. Flow cytometry was performed to assess human M2-like MΦ phenotype (CD14<sup>+</sup>CD80<sup>-</sup>CD206<sup>+</sup>/CD163<sup>+</sup>)

Mouse Bone Marrow (BM) isolation cells were collected from Lair1<sup>-/-</sup> and Lair1<sup>-/-</sup> C57/B6 mice and cultured with mouse M-CSF (PeproTech, 315-02-50) at a concentration of 100 ng/ml for 7 days. The culture medium was supplemented with 20 ng/ml mlL-4 (214-14), 20 ng/ml mlL-10 (210-10), 20 ng/ml mlL-13 (210-13) from PeproTech(4)in collagen I (5μg/ml, Millipore Sigma, CC050) and Collagen IV (5μg/ml, Millipore Sigma, CC076) coated plate for 48 hours. Western blotting was used to determine FXIII-A expression between *Lair1*<sup>-/-</sup> and *Lair1*<sup>-/-</sup> M2-like MΦ.

#### **FXIII-A Experiments**

BM-derived M2-like M $\Phi$  (2x10<sup>5</sup>/ml) were cultured with 10 µg/ml FXIII-A<sub>2</sub> protein (Zedira GmbH, T061) in Collagen I and Collagen IV (total 10µg/ml) coated plate for 48 hours. Flow cytometry was performed to assess human M2-like M $\Phi$  phenotype (CD45<sup>+</sup>CD11b<sup>-</sup>F4/80<sup>+</sup>Arg-1<sup>+</sup>). KR158B-CD70-Luc cells (1x10<sup>5</sup>/ml) were cultured with 10 µg/ml FXIII-A2 protein in Collagen I and Collagen IV (total 10µg/ml) coated plate for 24 hours, IF was performed to assess collagen IV expression.

#### In Vivo Imaging System (IVIS)

The process of IVIS was determined as described previously (1, 3). Briefly, Isoflurane-anesthetized animals were imaged using the IVIS system (Xenogen, Alameda, CA). The luminescent signal of Luciferase was detected 5 min after 50µl d-luciferin (PerkinElmer) injection intraperitoneally. The average radiant efficiency ([p/s/cm²/sr]/[µW/cm²]) within the ROI was used for quantitative fluorescence analysis. The average radiance (p/s/cm²/sr) within the ROI was used for all quantitative luminescence analyses.

## **Tumor-bearing (TB) Mice and Treatment**

TB mice were grouped based on IVIS measurements taken 1 day before treatment (-day 1, or -D1) to ensure similar initial tumor sizes. The average luminance ranged from 1×10⁴ to 1×10⁵, with comparable mean luminance across groups. aLAIR1 (R&D Systems, MAB100921) or IgG control

(R&D Systems, AB-105-C), the detailed information described in Functional antibodies, **Supplemental Table 1**. The mouse aLAIR1/IgG was administered via Intraperitoneal (i.p.) injection at a dose of 200 μg every other day from day 0 to day 8, 5 doses total. For the combination therapy, TB mice received 5 Gy total body irradiation on -day 1, followed by an intravenous (i.v.) injection of 1×10<sup>7</sup> CD70CAR T cells on day 0, with aLAIR1 administered at 200 μg/dose every other day from day 1 to day 9, 5 doses in total. For the L2-8R-70CAR and 8R-70CAR treatments, TB mice received 5 Gy total body irradiation on -day 1, followed by two intravenous i.v. injections of 1×10<sup>7</sup> CAR T cells on days 0 and 3. The tumor increases were calculated based on the baseline (Luminance -D1) of each mouse. e.g., The tumor increases on day 28 were calculated using the formula: (Luminance D28 - Luminance -D1)/ Luminance -D1 x 100%. The survival of TB mice was monitored per veterinary recommendations, and partial blinding was implemented in the study. Across all mouse models (KR158B-Luc, GL261-Luc, LLC1, and KR158B-CD70-Luc), no significant changes in body weight were observed during the initial two weeks (or four weeks for the KR158B-CD70-Luc model) following treatment.

### **Timepoints For Tissue Collection from Mice**

Aside from the endpoint of each TB mouse, tumor tissues were collected based on measurements obtained through IVIS imaging for brain tumors or calipers for LLC1 tumors, following the observation of noticeable trends of differences among the groups. Specifically, tumor tissues from KR158B-Luc TB mice were collected within 32±7 days, from KR158B-CD70-Luc mice within 42±7 days, and from LLC1 tumors within 12±3 days.

## 3D In Vitro Immunotherapy Assay

The 3D in vitro immunotherapy assay (iVITA) for evaluating cancer-immune interactions has been previously described (5). Briefly, tumor spheroids were generated by homogeneously mixing suspended cancer cells (4x10<sup>3</sup> cells/well) with inert liquid-like solid (LLS) microgels and culturing

them in a Darcy plate under continuous perfusion (6). Tumor spheroids began forming within 48 hours and matured by day 7. To facilitate cell adhesion and migration, we employed collagen type I (COL1-LLS) bio-conjugated microgels using EDC-NHS chemistry(5-7). A defined ratio (5:1) of M2-like MΦ to CAR or NAS T (8x10<sup>3</sup>:1.6x10<sup>3</sup>/well) cells was uniformly distributed around the tumor by homogenizing the cells at a selected concentration in COL1-LLS and depositing the mixture into a glass-bottom 96-well plate. Next, a custom-built Nikon Stage Mount 3D bioprinting micromanipulator (BioPelle™; Aurita Bioscience, BPLE NKN FC) was used to precisely position the solid tumor models within the working distance of the Nikon A1R confocal objective (20 X /0.75, Nikon Plan Apo VC). The plate was then centrifuged at 100xg with gentle acceleration and deceleration settings. Following centrifugation, growth media was carefully added, and the plate was secured in a custom-made stage incubator (Microscope Incubator, Aurita Bioscience, INC NKN STD) on a Nikon A1R confocal microscope equipped with a high-definition Galvano scanner for long-term in situ imaging. The co-cultures were maintained in incubators at 37°C and 5% CO2. Using the iVITA platform, we successfully captured and quantified key T cell functions, including trafficking, T cell/M2-like MΦ interactions, T cell/tumor interaction or infiltration, and tumor area analysis (5). For tracking and quantification, the entire confocal z-stack (150 µm range, step size: 2.4 µm) was reviewed to ensure uniform 3D distribution of T cells and M2-like MΦ surrounding the tumor at each 1-hour imaging interval. Maximum intensity projections of the time lapse were created, and individual channels were analyzed using FIJI (version 2.9.0/1.53t). The channels included red (excitation: 561 nm, emission: 570-616 nm) for T cells labeled with CellTracker™ Orange CMRA (Thermo Fisher Scientific, C34551), green (excitation: 488 nm, emission: 500-550 nm) for M2-like MΦ (labeled with CellTracker™ Green CMFDA, Thermo Fisher Scientific, C7025), and tumors cells were not stained with a fluorescent reporter. Cell segmentation was performed using intensity thresholds to ensure at least 95% overlap between thresholded objects and cell signals. Small particles (0-20 µm<sup>2</sup> in the T-cell channel and 0-50 µm<sup>2</sup> in the M2-like MΦ and tumor channels) were excluded as noise. The percentage of T and M2-like

373

374

375

376

377

378

379

380

381

382

383

384

385

386

387

388

389

390

391

392

393

394

395

396

397

 $M\Phi$ ; CAR T and tumor interactions was calculated by normalizing the intersected areas (M2-like  $M\Phi$  vs. T cells, and T cells vs. tumors) to the total T cell area at each 1-hour interval. T cell migration was tracked using the FIJI TrackMate Linear Assignment Problem (LAP) tracker, with a maximum frame-to-frame linking distance and an allowable track segment gap closure of 150 μm.

## Chipcytometry

399

400

401

402

403

404

405

406

407

408

409

410

411

412

413

414

415

416

417

418

419

420

421

422

Chipcytometry procedure was performed by Canopy Biosciences (Hannover, Germany). Tissue cryo-sections were prepared on a cryostat (NX50) with a thickness of 7 µm and stored overnight at -80°C before fixation in ice-cold acetone for 5 min, followed by 3 min of 90% and 70% EtOH, respectively. Fixed tissue sections were rinsed in PBS for 6 min and then loaded onto tissue chips. The chips were filled with storage buffer and stored at 4°C. Chips were rinsed with washing buffer for the staining procedure, and tissue autofluorescence was imaged in the FS560 channel. The autofluorescence images were used to assess tissue structure and integrity and to select regions of interest. The Chipcytometry assay consists of iterative staining, imaging, and photo-bleaching cycles. The three steps are repeated until all desired markers have been stained and imaged. After initial bleach and background imaging, antibodies were diluted from their stock solution in storage buffer to a total volume of 600 µl and briefly mixed according to the stain plan shown in the legend of Supplemental Figure 5. The antibody working solution was then pipetted dropwise into the liquid adapter of the chip, taking care not to introduce air bubbles into the chip. The chip was incubated for 15 min at room temperature before the working solution was flushed by pipetting 1 mL of storage buffer into the chip and then washed with 3 x 5 mL wash buffer with 2-5 min pause between wash steps. After washing, the chips were immediately put on the ZellScanner ONE instrument (Canopy Biosciences) and imaged, completing the cycle. This procedure followed the

stain plan outlined in the legend of **Supplemental Figure 5** until all markers were stained. Image data were processed and analyzed using the ZellExplorer Application (Canopy Biosciences).

#### **Cytokine Production**

423

424

425

426

427

428

429

430

431

432

433

434

435

436

437

438

439

440

441

442

443

444

445

446

To assess the cytokine release in the 3D culture, the culture supernatants were harvested and assayed 72 hours later by the multiplexing analysis performed by Eve Technologies Corp. (Calgary, Alberta) on the Luminex<sup>™</sup> 200 system (Luminex). Briefly, markers were simultaneously measured in the samples using Human Cytokine 48-Plex Discovery Assay® manufactured by Millipore Sigma. Individual analyte sensitivity values are available in the MILLIPLEX® MAP protocol. Individual ELISA was performed in-house using kits purchased from Thermo Fisher Scientific to confirm the results obtained above (G-CSF: BMS2001INST and CCL3: 88-7035-22). To evaluate the functionality of aLAIR1 in counteracting M2-like MΦ-mediated T-cell suppression in vitro using a 2D culture system. A flat-bottom 96-well plate was coated overnight at 4 °C with a collagen I/IV (10 µg/ml). The plate was then washed and air-dried at room temperature. 8R-CD70CAR T cells and M2-like MΦ were derived from the same human blood donor. 8R-CD70CAR T cells were co-cultured with M2-like MΦ and U87 GBM line at a ratio of M2-like MΦ: 8R-70CAR T: Tumor=5:1:2.5 (2x10<sup>5</sup>:4x10<sup>4</sup>: 1x10<sup>5</sup>) overnight, in the presence or absence of IgG or aLAIR1 (5 μg/ml) IFN-y assays were performed by ELISA (Thermo Fisher Scientific, KHC4021). The LAIR2 release from L2-8R-70CAR T cells at multiple time points was determined by ELISA (R&D Systems, DY2665). To evaluate the anti-tumor effect of L2-8R-70CAR and 8R-70CAR T cells in human, the CAR T cells were co-cultured overnight with U87/pGBM#1 at a ratio of 1:1 (1x10<sup>5</sup>). IFN-y assays were performed by ELISA. To evaluate the anti-tumor effect of L2-8R-70CAR and 8R-70 CAR T cells in mice, the CAR T cells were co-cultured overnight with KR158B-CD70-Luc/KR158B-Luc at a ratio of 1:1 (1x10<sup>5</sup>: 1x10<sup>5</sup>). IFN-y assays were performed by ELISA (Thermo Fisher Scientific, BMS606).

## **Antibody Binding Evaluation**

447

448

449

450

451

452

453

454

455

456

457

458

459

460

461

462

463

464

465

466

467

468

469

470

471

Functional ELISA was performed to evaluate whether Human aLAIR1 inhibits LAIR1-collagen interaction. Firstly, increasing concentrations (0.002, 0.005, 0.009, 0.19, 0.38, 0.75, 1.5, 3, 6, 12, 24, 48, 96, 192µg/ml) of human LAIR1-His tag protein (R&D systems, 2664-LR) were incubated on collagen I/IV-coated plates (10µg/ml) for 2 hours at room temperature. Binding was quantified by His-tag ELISA, a reagent from R&D systems (BAM050, DY994, DY998, DY999), and EC<sub>50</sub> was identified. Then 1µg/ml (approximately value of EC<sub>50</sub>) LAIR1-His protein was pre-incubated with increasing concentrations (0.013, 0.025, 0.05, 0.1, 0.2, 0.4, 0.8, 1.59, 3.18, 6.25, 12.5, 25, 50, 100, 200, 400µg/ml) of human aLAIR1(Hycult biotech, HM2364) or IgG (Hycult biotech, HI1016) for 1 hour, then added to uncoated plates for 2 hours. Three collagen-coated wells served as maximal (Max, 100%) binding controls. Binding was quantified by His-tag ELISA and reported as % response relative (% to Max) to the LAIR1-only collagen-coated control. Finally, aLAIR1 or IgG was pre-incubated with LAIR1-His, as described above, followed by incubation on collagen I/IV-coated plates for 2 hours at room temperature. Binding was quantified by His-tag ELISA. The inhibition was calculated as 100% minus the relative response (%), i.e., Inhibition = 100% - % response relative. The IC<sub>50</sub> value was calculated by nonlinear regression using a four-parameter logistic model.

#### Flow Cytometry

For fluorescent conjugated antibodies surface staining, cells were stained with various markers at room temperature for 15 min, washed with PBS, and resuspended in PBS containing 1:1000 dilution of LIVE/DEAD™ Fixable Dead Cell Stain Kit (Thermo Fisher Scientific, C34557). Washed once and resuspended in FACS buffer (PBS with 2% fetal calf serum) before analysis on a flow cytometer. For intracellular/intranuclear staining, such as Arg-1, cells were first labeled with LIVE/DEAD™ Fixable Dead Cell Stain Kit as described above. Cells were then fixed/permeabilized using the Foxp3 Transcription Factor Staining Buffer Set (Thermo Fisher

Scientific, 00-5523-00) for 1 hour at 4 °C and were stained with the surface maker and Arg-1 antibodies (Thermo Fisher Scientific, 25-3697-82). To evaluate the Gramz B and TNF-α in T cells, the cells were cultured with GolgiStop (BD, 554724, 0.67μl/ml) in 37 °C incubator for 6 hours, followed by fixed/permeabilized using the Foxp3 Transcription Factor Staining Buffer Set for 1 hour at 4 °C and were stained with the surface maker and intracellular antibodies. Detailed information on antibodies is presented in **Supplemental Table 1**. All the samples were analyzed using Canto II<sup>TM</sup> Flow Cytometer, and acquired data were analyzed using FlowJo software version 10.8.1. Gating strategies are displayed in above.

## **T-cell Proliferation Assay**

T-cell proliferation was evaluated using flow cytometry following 3 days of stimulation with anti-CD3/anti-CD28 Dynabeads (Thermo Fisher Scientific). A flat-bottom 96-well plate was coated overnight at 4 °C with a collagen I & IV mixture (Sigma, total 10  $\mu$ g/ml). The plate was then washed and air-dried at room temperature. T cells were stained with CellTrace Violet (Thermo Fisher Scientific, C34557) and co-cultured with M2-like M $\Phi$  derived from the same donor's PBMCs. The cells were added to each well at a 5:1 ratio (2 × 10 $^{5}$  M2-like M $\Phi$ : 4 × 10 $^{4}$  T cells per well). Anti-CD3/anti-CD28 Dynabeads (Thermo Fisher Scientific) were included at a 1:1 T-cell-to-bead ratio, with 4 × 10 $^{4}$  beads per well. Daily treatments included aLAIR1, IgG control (Hycult Biotech, 5  $\mu$ g/ml), LAIR1 agonist ( $\underline{8}$ ) (BD, 550810, 5  $\mu$ g/ml), or PBS (Thermo Fisher Scientific, 10  $\mu$ l). After 3 days of culture, T-cell proliferation was assessed by Flow Cytometry (gating on CD3+Celltrace-).

## **Cell Apoptosis Elevation**

To elevate the function of haLAIR1 on LAIR1 $^+$  cells, the THP-1 cells and PBMC-induced M2-like M $\Phi$  (1x10 $^5$ /ml) were cultured with 5 µg/ml of IgG or aLAIR1 for 3 days in a collagen I/IV coated plate. Flow cytometry assessed these cells' viability using Annexin V (Biolegend, 640941) and

Propidium Iodide (PI, Thermo Fisher Scientific, P1304MP). Annexin V<sup>+</sup>PI<sup>-</sup> cells represent early apoptosis cells, and Annexin V<sup>+</sup>PI <sup>+</sup> cells are late apoptosis cells.

498

499

500

501

502

503

504

505

506

507

508

509

510

511

512

513

514

515

516

517

518

519

520

497

496

## In-house Single-Cell RNA Sequencing and Data Analysis

Tumor single-cell suspensions were first washed with PBS, and their viability was confirmed through Trypan Blue staining. These suspensions were subsequently labeled and combined using the 3' CellPlex Kit Set A. Following this, they were loaded onto the Chromium Single Cell Chip G (10x Genomics) as per the manufacturer's guidelines, aiming for a target capture rate of approximately 30,000 cells per sample. The pooled single-cell RNA-seq libraries were then prepared according to the manufacturer's instructions, utilizing the Chromium Single Cell 3' V3.1 Solution (10x Genomics). All single-cell cDNA was divided into two types of libraries: 3' Gene Expression libraries and Cell Multiplexing libraries. Both library types were subjected to pairedend, dual indexing sequencing (SI-TT for gene expression and SI-NN for multiplexing) on the Illumina Novaseq platform. This sequencing process included a 28-base read 1 containing cell barcodes and unique molecular identifiers (UMI) and a 150-base read 2 for mRNA insert. The sequencing depth aimed to achieve more than 20,000 read pairs per cell for gene expression and 5,000 read pairs per cell for multiplexing. The data were analyzed by the Department of Neurosurgery at the University of Florida using the same analysis method. The demultiplexed cells were aligned to the mouse mm10 genome using Cellranger 7.0 (10x genomics). Subsequently, the data was analyzed using Seurat 4.0 (9). The analysis began with quality control metrics, where cells were assessed based on mRNA count (>250), barcodes per cell (>500), cell complexity (log10GenesPerUMI > 0.80), and percentage of mitochondrial genes (<20%). SingleR v.2.4.1 was employed for cell cluster deconvolution, utilizing cell type signature genes obtained from the differentially expressed genes (DEGs) within the clusters (10). Moreover, CellChat 2.1.0 was utilized to explore cell-to-cell interactions (11). To identify differentially expressed genes

(DEGs) on specific cell types between groups, the Limma-voom 3.58.1 method was employed (12). Subsequently, ggplot2 3.4.1 was used to generate relevant plots (13).

# **Western Blotting**

The BM and M2-like MΦ cells were treated with a RIPA buffer (Thermo Fisher Scientific, 89900) containing a cocktail of Protease and Phosphatase Inhibitor Cocktail (Thermo Fisher Scientific, 78440) and placed on ice for 20 min and then centrifuged the samples at 4°C at 13,000 x g for 15 min. The lysate supernatant was collected, and the protein concentration was determined by Pierce™ BCA Protein Assay Kits (Thermo Fisher Scientific, 23225). The same amount of proteins was analyzed by SDS-PAGE (Bio-Red) and transferred to polyvinylidene fluoride (PVDF) membranes (Thermo Fisher Scientific, 88518). The membrane was blocked in TBST (Thermo Fisher Scientific, J77500.K2) with Superblock buffer (Thermo Fisher Scientific, 37515) for 1 h and then kept at 4°C overnight with anti-FXIII-A1 primary antibody (Santa Cruz Biotechnology, sc-271122, 1:100). Detailed information of antibodies is presented in **Supplemental Table 1**. The membrane was then washed with TBST at least 3 times and incubated at room temperature with goat-anti-rabbit IgG HRP (R&D systems, HAF09, 1:500) for 1 hour before exposure and photography.

#### Immunofluorescence

Immunofluorescence (IF) was performed for CD45, Tmem119, LAIR1, EGFR, collagen I, collagen IV expression, CD8, and CXCR2. Tumor brain samples from humans or mice were freshly embedded in OCT, slowly frozen in a slush of dry ice and 95% alcohol, and then cryosectioned (5 or 10 μm). Sections were incubated with Superblock buffer with 0.2% Triton X-100 (Thermo Fisher Scientific, A16046.AE) for 1 hour before staining and stained with primary antibodies: rabbit anti-human LAIR1 (Cell Signaling, 60061, 1:100); rat anti-human CD45 (Thermo Fisher Scientific,

MA5-17687, 1:100); mouse anti-human EGFR (Thermo Fisher Scientific, MA5-13070, 1:200); mouse anti-human Tmem119 (Cell Signaling, 41134, 1:50), Rabbit anti-mouse collagen I (R&D Systems, NB600-408, 1:100), rabbit anti-mouse collagen IV (Abcam, ab19808, 1:100), Rabbit anti-human CXCR2 (Gene Tex, GTX639056, 1:50), Rat anti-mouse CD8 (Thermo Fisher Scientific, MA1-145, 1:100) at 4 °C for overnight, followed by secondary antibodies coupled with a fluorophore (goat anti-rabbit IgG-Alexa Fluor488, and goat anti-rat IgG- Fluor568, Goat antimouse IgG-Alexa Fluor647, Thermo Fisher Scientific, 1:500) at room temperature for 1 h. Detailed information on antibodies is presented in **Supplemental Table 1.** DAPI (Thermo Fisher Scientific, D1306) was used for nuclei staining. Additional sections were prepared and stained with flourconjugated secondary antibodies only to confirm the specificity of the primary antibodies for their indicated epitopes. Images were acquired using a Nikon A1RMP Confocal Microscope, using the following visible excitation lasers (405nm, 488nm, 561nm, and 647nm) and emission filter bands (450/50, 525/50, 595/50, 700/75). Mono-LASER based segregated stepwise image acquiring algorithm set up as default from LASERs 405nm, 488nm, 561nm, and 647nm to minimize spectral spillover between channels. For imaging quantitation, density analysis was performed with Fiji/ImageJ Software (14). Voxel-based co-localization as well as 3D reconstruction of the confocal images was performed using the Imaris Cell Imaging Software x 64 9.7.0 (Oxford Instruments). For imaging cell number analysis was performed using Qupath-0.5.1 software. To determine if LAIR1 is on tumor-infiltrating MΦ or resident microglia, CD45<sup>+</sup> cells were divided into CD45<sup>high</sup> (top 50%) and CD45<sup>low</sup> (bottom 50%) populations. The Collagen I & IV levels (measured as mean fluorescence intensity, MFI) were calculated by the formula: (Total intensity -Background intensity)/ Total nuclei. The % of CAR T cell infiltration was calculated by the formula: Total mouse CD8<sup>+</sup> and human CXCR2<sup>+</sup> double-positive cells/ Total nuclei.

544

545

546

547

548

549

550

551

552

553

554

555

556

557

558

559

560

561

562

563

564

565

566

| 567        | Immunohistochemistry (IHC) of Cancer Tissues   |
|------------|--|
| 568        | The IHC images of tumor tissues were acquired from the Human Protein Atlas, version 23.0 |
| 569        | (https://www. proteinatlas.org/) (15). The original images can be found:                 |
| 570        | Colorectal Cancer: Patient ID: 693   |
| 571        | https://www.proteinatlas.org/ENSG00000167613-LAIR1/cancer/colorectal+cancer#             |
| 572        | Lung Cancer: Patient ID: 2222  |
| 573        | https://www.proteinatlas.org/ENSG00000167613-LAIR1/cancer/lung+cancer#img                |
| 574        | Melanoma: Patient ID: 2534   |
| 575        | https://www.proteinatlas.org/ENSG00000167613-LAIR1/cancer/melanoma#img                   |
| 576        | Ovarian Cancer: Patient ID: 2391   |
| 577        | https://www.proteinatlas.org/ENSG00000167613-LAIR1/cancer/ovarian+cancer#img             |
| 578        | Renal Carcinoma: Patient ID: 1481  |
| 579        | https://www.proteinatlas.org/ENSG00000167613-LAIR1/cancer/renal+cancer#img               |
| 580        | Stomach Cancer: Patient ID: 2142   |
| 581        | https://www.proteinatlas.org/ENSG00000167613-LAIR1/cancer/stomach+cancer#img             |
| 582        | Testis Cancer: Patient ID: 1777  |
| 583        | https://www.proteinatlas.org/ENSG00000167613-LAIR1/cancer/testis+cancer#img              |
| 584        | Lymphoma: Patient ID: 1734   |
| 585<br>586 | https://www.proteinatlas.org/ENSG00000167613-LAIR1/cancer/lymphoma#img                   |

# 587 Supplemental Table 1. Antibodies used in this study

| ANTIBODIES                                | PROVIDER                    | IDENTIFIER  | APPLICATION        |
|---|-----------------------------|---|--------------------|
| Functional antibodies                     |                             |   |                    |
| Mouse anti-human<br>LAIR1                 | Hycult biotech              | Cat# HM2364<br>Clone: NKTA255<br>RRID:100ugAB_2942<br>052 | LAIR1 Blockade     |
| Rabbit anti-mouse LAIR1                   | R&D Systems                 | Cat# MAB100921<br>Clone: 2459B<br>RRID: AB_3657110        | LAIR1 Blockade     |
| Rat anti-mouse PD-1                       | BioXCell                    | Cat# BE0146<br>Clone: RMP1-14<br>RRID: AB_10949053        | PD-1 Blockade      |
| Mouse IgG                                 | Hycult biotech              | Cat# HI1016-50ug<br>Clone: MOPC-21<br>RRID: AB_2942051    | Control            |
| Rabbit IgG                                | R&D Systems                 | Cat# AB-105-C<br>Clone: 2459B<br>RRID: AB_354266          | Control            |
| Mouse anti-human<br>LAIR1 (LAIR1 agonist) | BD                          | Cat# 550810<br>Clone: DX26<br>RRID: AB_393895             | LAIR1 agonist      |
| Ultra-LEAF™ Purified<br>Anti-mouse CD3ε   | Biolegend                   | Cat# 100340<br>Clone: 145-2C11<br>RRID: AB_11149115       | T cell stimulation |
| Ultra-LEAF™ Purified<br>Anti-mouse CD28   | Biolegend                   | Cat# 102116<br>Clone: 37.51<br>RRID: AB 11147170          | T cell stimulation |
| Detecting antibodies                      |                             | _   |                    |
| Rat anti-human CD45                       | Thermo Fisher<br>Scientific | Cat# MA5-17687;<br>Clone: YAML501.4<br>RRID: AB 2539077   | IF (1:100)         |
| Rabbit anti-human LAIR1                   | Cell Signaling              | Cat# 60061<br>Clone: E7X6I<br>RRID: AB_2238514            | IF (1:100)         |
| Mouse anti-Human<br>Tmem119               | Cell Signaling              | Cat # 41134<br>Clone: E3E4T<br>RRID: AB_3094467           | IF (1:50)          |
| Mouse anti-human<br>EGFR                  | Thermo Fisher<br>Scientific | Cat# <b>MA5-13070</b><br>Clone: H11<br>RRID: AB 10977527  | IF (1:200)         |
| Anti-mouse CD8                            | Thermo Fisher<br>Scientific | Cat# 11-0081-82<br>Clone: 53-6.7<br>RRID: AB 464915       | IF (1:100)         |
| Rabbit anti-mouse<br>Collagen IV          | Abcam                       | Cat# ab19808<br>Clone: COL4A1<br>RRID: AB_445160          | IF (1:100)         |
| Rabbit anti-human CXCR2                   | Gene Tex                    | Cat# GTX639056<br>Clone: HL2604                           | IF (1:50)          |

| Rat anti-mouse CD8     | Thermo Fisher | Cat# MA1-145      | IF (1:100)  |
|------------------------|---------------|-------------------|-------------|
| rat and mouse obo      | Scientific    | Clone: 2.43       | 11 (1.100)  |
|                        | Ocientino     | RRID: AB 2536854  |             |
| PerCP/Cyanine5.5       | BD            | Cat# 551163       | FC (1:100)  |
| hamster anti-mouse CD3 | DD            | Clone: 145-2C11   | 1 8 (1.100) |
| Hamster anti-mouse CD3 |               | RRID: AB_394082   |             |
| APC rat anti-mouse     | BD            | Cat# 559864       | FC (1:100)  |
| CD45                   | טט            | Clone: 30-F11     | 1 C (1.100) |
| GD43                   |               | RRID: AB 398672   |             |
| PE/Cyanine7 rat anti-  | Biolegend     | Cat# 103114       | FC (1:100)  |
| mouse CD45             | biolegena     | Clone: 30-F11     | 1 C (1.100) |
| mouse ob45             |               | RRID: AB 312979   |             |
| APC rat anti-mouse     | BD            | Cat# 561018       | FC (1:100)  |
| CD45                   | טט            | Clone: 30-F11     | 1 C (1.100) |
| CD43                   |               | RRID: AB 398672   |             |
| APC/Cyanine7 rat anti- | BD            | Cat# 557659       | FC (1:100)  |
| mouse CD45             | טט            | Clone: 30-F11     | 1 C (1.100) |
| mouse ob45             |               | RRID: AB 396774   |             |
| PerCP/Cyanine5.5 rat   | BD            | Cat# 561114       | FC (1:100)  |
| anti-mouse CD11b       | טט            | Clone: M1/70      | 1 C (1.100) |
| anti-mouse CD11b       |               | RRID: AB 2033995  |             |
| APC/Cyanine7 anti-     | Biolegend     | Cat# 123118       | FC (1:100)  |
| mouse F4/80            | biolegena     | Clone: BM8        | FC (1.100)  |
| House F4/00            |               | RRID: AB 893489   |             |
| PE Armenian hamster    | Thermo Fisher | Cat# 12-3051-82   | FC (1:100)  |
| anti-mouse LAIR1       | Scientific    | Clone: 113        | FC (1.100)  |
| anti-mouse LAIN        | Scientific    | RRID: AB 1210738  |             |
| PE-Cyanine7 rat anti-  | Thermo Fisher | Cat# 25-3697-82   | FC (1:100)  |
| mouse Arg-1            | Scientific    | Clone: A1exF5     | FC (1.100)  |
| mouse Arg-1            | Scientific    | RRID: AB 2734841  |             |
| PE-Cyanine7 rat anti-  | BD            | Cat# 552775       | FC (1:100)  |
| mouse CD4              | טט            | Clone: RM4-5      | FC (1.100)  |
| mouse CD4              |               | RRID: AB 394461   |             |
| anti-mouse CD70        | BD            | Cat# 555286       | FC (1:100)  |
| anti-mouse CD70        | טט            | Clone: FR70       | FC (1.100)  |
|                        |               | RRID: AB 395705   |             |
| APC/Cyanine7 anti-     | Biolegend     | Cat# 301820       | FC (1:100)  |
| human CD14             | biolegena     | Clone: M5E2       | 1 C (1.100) |
| Haman OD 14            |               | RRID: AB 493695   |             |
| PE/Cyanine7 anti-human | Biolegend     | Cat# 321124       | FC (1:100)  |
| CD206                  | Diologena     | Clone: 15-2       | 1 5 (1.100) |
|                        |               | RRID: AB 10933248 |             |
| APC anti-human CD163   | Biolegned     | Cat# 333610       | FC (1:100)  |
| 7. Cana haman Ob 100   | Biologilod    | Clone: GHI/61     | (1.100)     |
|                        |               | RRID: AB 2291272  |             |
| PE-Cyanine7 moue anti- | Biolegned     | Cat# 368532       | FC (1:100)  |
| human CD45             | Biologilod    | Clone: 2D1        | (1.100)     |
| Haman ODTO             |               |                   |             |
|                        |               | RRID: AB 2715892  |             |

| BV421 mouse anti-<br>human CD3        | BD                          | Cat# 563798<br>Clone: SK7<br>RRID: AB_2744383          | FC (1:100) |
|---------------------------------------|-----------------------------|--|------------|
| APC mouse anti-human CD70             | Biolegned                   | Cat# 355110<br>Clone: 113-16<br>RRID: AB_2562481       | FC (1:100) |
| FITC mouse anti-human CXCR2           | Biolegend                   | Cat# 320704<br>Clone: 5E8/CXCR2<br>RRID: AB 439805     | FC (1:100) |
| PE Mouse anti-human<br>LAIR1          | Thermo Fisher<br>Scientific | Cat# 12-3059-42<br>Clone: NKTA255<br>RRID: AB_11042284 | FC (1:100) |
| PE mouse anti-Human<br>Granzyme B     | BD                          | Cat# 561142<br>Clone: GB11<br>RRID: AB_10561690        | FC (1:100) |
| PE-Cyanine7 moue anti-<br>human TNF-a | Biolegend                   | Cat# 502930<br>Clone: MAb11<br>RRID: AB_2204079        | FC (1:100) |
| Mouse anti FXIII-A                    | Santa Cruz<br>Biotechnology | Cat# sc-271122<br>Clone: A-4<br>RRID: AB 10608225      | WB (1:100) |
| Goat anti-rabbit IgG HRP              | R&D Systems                 | Cat# HAF008<br>RRID: AB_357235                         | WB (1:500) |
| Goat anti-rabbit Alexa<br>Fluor 488   | Thermo Fisher<br>Scientific | Cat# A-11034<br>RRID: AB_2576217                       | IF (1:500) |
| Goat anti-rabbit Alexa<br>Fluor 568   | Thermo Fisher<br>Scientific | Cat# A-11011<br>RRID: AB_143157                        | IF (1:500) |
| Goat anti-rat Alexa Fluor 568         | Thermo Fisher<br>Scientific | Cat# A-11077<br>RRID: AB_2534121                       | IF (1:500) |
| Goat anti-mouse Alexa<br>Fluor 647    | Thermo Fisher<br>Scientific | Cat# A-21235<br>RRID: AB_2535804                       | IF (1:500) |
| Goat anti-Hamster Alexa<br>Fluor 674  | Thermo Fisher<br>Scientific | Cat# A-21451<br>RRID: AB_2535868                       | IF (1:500) |

Note: IF: Immunofluorescence, FC: Flow Cytometry, WB: Western Blotting

## 589 **Reference**

590

- 591 1. Jin L, Tao H, Karachi A, Long Y, Hou AY, Na M, et al. CXCR1- or CXCR2-modified CAR 592 T cells co-opt IL-8 for maximal antitumor efficacy in solid tumors. *Nature Communications*. 593 2019;10(1):4016.
- 594 2. Song R, Bafit M, Tullett KM, Tan PS, Lahoud MH, O'Keeffe M, et al. A Simple and Rapid 595 Protocol for the Isolation of Murine Bone Marrow Suitable for the Differentiation of 596 Dendritic Cells. *Methods and Protocols*. 2024;7(2):20.
- Jin L, Ge H, Long Y, Yang C, Chang YE, Mu L, et al. CD70, a novel target of CAR T-cell therapy for gliomas. *Neuro Oncol.* 2018;20(1):55-65.
- 599 4. Zarif JC, Hernandez JR, Verdone JE, Campbell SP, Drake CG, and Pienta KJ. A phased 600 strategy to differentiate human CD14+monocytes into classically and alternatively 601 activated macrophages and dendritic cells. *Biotechniques*. 2016;61(1):33-41.

- 602 5. Nguyen DT, Liu R, Ogando-Rivas E, Pepe A, Pedro D, Qdaisat S, et al. Bioconjugated 603 liquid-like solid enhances characterization of solid tumor - chimeric antigen receptor T cell 604 interactions. *Acta Biomater*. 2023;172:466-79.
- 605 6. Nguyen DT, Famiglietti JE, Smolchek RA, Dupee Z, Diodati N, Pedro DI, et al. 3D In Vitro Platform for Cell and Explant Culture in Liquid-like Solids. *Cells*. 2022;11(6).
- 7. Nguyen DT, Pedro DI, Pepe A, Rosa JG, Bowman JI, Trachsel L, et al. Bioconjugation of COL1 protein on liquid-like solid surfaces to study tumor invasion dynamics. Biointerphases. 2023;18(2):021001.
- 610 8. Meyaard L, Adema GJ, Chang C, Woollatt E, Sutherland GR, Lanier LL, et al. LAIR-1, a 611 Novel Inhibitory Receptor Expressed on Human Mononuclear Leukocytes. *Immunity*. 612 1997;7(2):283-90.
- Hao Y, Hao S, Andersen-Nissen E, Mauck WM, Zheng S, Butler A, et al. Integrated analysis of multimodal single-cell data. *Cell.* 2021;184(13):3573-87.e29.
- 615 10. Aran D, Looney AP, Liu L, Wu E, Fong V, Hsu A, et al. Reference-based analysis of lung single-cell sequencing reveals a transitional profibrotic macrophage. *Nature Immunology*. 2019;20(2):163-72.
- 518 11. Jin S, Guerrero-Juarez CF, Zhang L, Chang I, Ramos R, Kuan C-H, et al. Inference and analysis of cell-cell communication using CellChat. *Nature Communications*. 2021;12(1):1088.
- Law CW, Chen Y, Shi W, and Smyth GK. voom: precision weights unlock linear model analysis tools for RNA-seq read counts. *Genome Biology*. 2014;15(2):R29.
- 623 13. Wickham H, and Wickham H. *Data analysis*. Springer; 2016.

628

- 624 14. Schneider CA, Rasband WS, and Eliceiri KW. NIH Image to ImageJ: 25 years of image analysis. *Nature Methods*. 2012;9(7):671-5.
- Uhlén M, Fagerberg L, Hallström BM, Lindskog C, Oksvold P, Mardinoglu A, et al. Tissue-based map of the human proteome. *Science*. 2015;347(6220):1260419.